

Aus der Klinik und Poliklinik für Frauenheilkunde und Geburtshilfe

Klinikum der Ludwig-Maximilians-Universität München

Vorstand: Prof. Dr. Sven Mahner



***Epigenome and transcriptome changes in Assisted
Reproductive Techniques (ARTs)***

Dissertation

zum Erwerb des Doktorgrades der Humanbiologie

an der Medizinischen Fakultät der

Ludwig-Maximilians-Universität München

vorgelegt von

Huixia Yang

aus

Shandong, China

Jahr

2022

Mit Genehmigung der Medizinischen Fakultät der
Ludwig-Maximilians-Universität zu München

Erster Gutachter: Prof. Dr. Udo Jeschke

Zweiter Gutachter: Prof. Dr. Artur Mayerhofer

Dritter Gutachter: Prof. Dr. Axel Imhof

Mitbetreuung durch den
promovierten Mitarbeiter: Dr. Viktoria von Schönfeldt

Dekan: Prof. Dr. med. Thomas Gudermann

Tag der mündlichen Prüfung: 12.10.2022

Affidavit



Affidavit

Yang, Huixia

Surname, first name

Maistraße 11

Street

80337, Munich, Germany

Zip code, town, country

I hereby declare, that the submitted thesis entitled:

Epigenome and transcriptome changes in Assisted Reproductive Techniques (ARTs)

is my own work. I have only used the sources indicated and have not made unauthorised use of services of a third party. Where the work of others has been quoted or reproduced, the source is always given.

I further declare that the dissertation presented here has not been submitted in the same or similar form to any other institution for the purpose of obtaining an academic degree.

Munich, 21.04.2022

place, date

Huixia Yang

Signature doctoral candidate

Table of content

Affidavit	3
Table of content	4
List of abbreviations	5
List of publications	6
1. Contribution to the publications	7
1.1 Contribution to paper I.....	7
1.2 Contribution to paper II.....	7
2. Introduction	8
2.1 The epigenome changes in the ART offspring	9
2.2 The epigenome changes in the ART placenta	11
2.3 Transcriptome changes in aging oocytes.....	14
2.4 Introduction to epigenome and transcriptome	15
2.5 Aim of the study	17
3. Summary (English)	19
4. Zusammenfassung (Deutsch)	22
5. Paper I	25
6. Paper II	45
References	60
Acknowledgements	67
Curriculum vitae	69

List of abbreviations

ART	Assisted Reproductive Technologies
IVF	in vitro fertilization
ICSI	intracytoplasmic sperm injection
IVM	in vitro maturation
PGD	preimplantation genetic diagnosis
<i>DAZ</i>	<i>Deleted in Azoospermia</i>
BWS	Beckwith-Wiedemann syndrome
ICR	imprinting control region
<i>IGF2</i>	<i>Insulin Like Growth Factor 2</i>
<i>H19</i>	<i>H19 Imprinted Maternally Expressed Transcript</i>
AS	Angelman Syndrome
<u><i>UBE3A</i></u>	<i>Ubiquitin Protein Ligase E3A</i>
<i>SNRPN</i>	<i>Small Nuclear Ribonucleoprotein Polypeptide N</i>
<i>PEG10</i>	<i>Paternally Expressed 10</i>
<i>MEST</i>	<i>Mesoderm Specific Transcript</i>
<i>L3MBTL1</i>	<i>L3MBTL Histone Methyl-Lysine Binding Protein 1</i>
<i>KCNQ1OT1</i>	<i>KCNQ1 Opposite Strand/Antisense Transcript 1</i>
GV	germinal vesicle
MII	metaphase II
HTA	Human Transcriptome Arrays
H3K4me3	tri-methylated-histone-H3-lysine-4
ChIP	Chromatin immunoprecipitation
TSS	transcription start site
mRNA	messenger RNA
tRNA	transfer RNA
rRNA	ribosomal RNA
ncRNA	non-coding RNA
<i>FAM111A</i>	<i>FAM111 Trypsin Like Peptidase A</i>

List of publications for cumulative dissertation

- *Comparison of Histone H3K4me3 between IVF and ICSI Technologies and between Boy and Girl Offspring (Paper I)*

Huixia Yang, Zhi Ma, Lin Peng, Christina Kuhn, Martina Rahmeh, Sven Mahner, Udo Jeschke, Viktoria von Schönfeldt. Comparison of Histone H3K4me3 between IVF and ICSI Technologies and between Boy and Girl Offspring. *Int J Mol Sci.* 2021 Aug 9;22(16):8574. doi: 10.3390/ijms22168574.

- *FAM111A Is a Novel Molecular Marker for Oocyte Aging (Paper II)*

Huixia Yang, Thomas Kolben, Mirjana Kessler, Sarah Meister, Corinna Paul, Julia van Dorp, Sibel Eren, Christina Kuhn, Martina Rahmeh, Cornelia Herbst, Sabine Gabriele Fink, Gabriele Weimer, Sven Mahner, Udo Jeschke, Viktoria von Schönfeldt. *FAM111A Is a Novel Molecular Marker for Oocyte Aging.* *Biomedicines.* 2022 Jan 25;10(2):257. doi: 10.3390/biomedicines10020257.

1. Contribution to the publications

1.1 Contribution to paper I

As the first author of paper I, Huixia Yang conducted:

- (1) sample size estimation;
- (2) clinical data collection and statistical analysis;
- (3) the experiments including immunohistochemistry on placentae, cell culture in various oxygen conditions, immunocytochemistry, knock-down experiment with small-interfering RNA, and Western blots;
- (4) ChIP-seq data processing and analysis;
- (5) data visualization;
- (6) manuscript writing, editing and revision.

1.2 Contribution to paper II

As the first author of paper II, Huixia Yang conducted:

- (1) RNA-seq data processing and analysis;
- (2) data visualization;
- (3) manuscript writing, editing and revision.

2. Introduction

Assisted Reproductive Technology (ART) has continued to advance in the recent decades since the birth of the first “test-tube” baby on 25 July 1978. ARTs mainly include in vitro fertilization (IVF), intracytoplasmic sperm injection (ICSI), in vitro maturation (IVM), preimplantation genetic diagnosis (PGD), cryopreservation of gametes and embryos, etc. The most popular, IVF, refers to the collection of oocytes from women's ovaries, and then fertilizing the eggs and maintaining them in vitro until the embryos are transferred into the uterine cavity. However, during the whole operation of IVF, the sperm do not spend a period of time residing in the female reproductive tract or undergoing capacitation. Less common, ICSI refers to microinjection of single sperm into the oocyte cytoplasm, and it is usually used in male oligospermia or asthenospermia or due to failed fertilization in previous IVF attempts. ICSI lacks the natural selection of human reproduction, presenting increased risk of chromosomal aberration, gene mutation, deletion, and epigenetic abnormalities in spermatozoa. For example, the deletion of the Y chromosomal *Deleted in Azoospermia (DAZ)* genes has been reported as related to azoospermia or oligozoospermia in humans [1]. Similarly, chromosomal abnormalities are five times more frequently found in male ICSI candidates in comparison to the normal population [2].

As of date, the clinical application of the various ART techniques has helped many infertility couples and resulted in more than 9 million births worldwide [3]. Moreover, it is estimated that the overall number of ART children will continue to grow due to delayed childbearing, adverse environmental exposure

and lifestyle-associated infertility [4]. Nevertheless, ART still faces several challenges such as (1) ART safety (ART as a technology is applied in the human clinical practice but without security verification) and (2) reproductive aging (oocyte aging is one of the main causes of ART failure, but to date, there is still far from a solution to this problem). Resolution of these challenges requires comprehensive and in-depth biology studies, especially investigations into epigenome and transcriptome and changes. Solving these problems would likely help increase the success rate of ART, as well as provide a basis for the treatment of ART children with epigenetic disorders and other cardiometabolic disorders, and pave the way for further development of ART.

2.1 The epigenome changes in the ART offspring

ART is a non-physiologic intervention, which can be reflected in the nature of procedures such as ovarian stimulation, in vitro manipulation of gametes, in vitro embryo culture, transfer, as well as the cryopreservation. Besides, ART intervention occurs at a sensitive period for gametogenesis, maturation, and early embryo development. During this period, the gamete/embryo undergoes extensive epigenetic reprogramming, and it has been revealed that ART manipulation may influence imprint establishment and imprint maintenance, as well as further affect the ART offspring's health [5]. Large-scale epidemiological studies have reported that the ART offspring have a higher ratio of preterm birth, low birth weight, birth defects, and infant mortality compared to those in natural pregnancy groups [6–8]. Moreover, it has also been suggested that ART-children have elevated risk of suffering imprinting diseases and aberrant epigenetic changes [9].

Among the reported imprinting defects, Beckwith-Wiedemann syndrome (BWS) is the most relevant to ART [10]. This is a pediatric overgrowth syndrome with increased susceptibility to tumors that results from methylation defects in the imprinting control region (ICR) of *Insulin Like Growth Factor 2 (IGF2)/Imprinted Maternally Expressed Transcript (H19)* [11, 12]. The key characteristics of BWS include macroglossia, abdominal wall defects and macrosomia [13]. According to a study from the UK [14], 4% of infants with BWS (6/149) were born as the result of IVF/ICSI, while, in the general population (n=4,320,482), only 0.997% of births were derived from IVF/ICSI. Angelman Syndrome (AS) is another common imprinting disorder investigated within the context of ART, and it is characterized by particular facies and growth and development delays [15]. AS is a neuro-developmental disorder that results from mutations or deletions in the chromosome 15 and is usually associated with the loss or mutation of the *Ubiquitin Protein Ligase E3A (UBE3A)* gene [16]. Besides these, some imprinted genes also present aberrant epigenetic status in ART offspring. For instance, Whitelaw et al. [17] analyzed the DNA methylation level in genes from the buccal cells of IVF-children (mean age 2.90 years), ICSI-children (mean age 2.70 years), and natural conception-children (mean age 2.81 years), and they found the imprinted gene *Small Nuclear Ribonucleoprotein Polypeptide N (SNRPN)* in the ICSI-children presented significantly higher DNA methylation levels compared with that from natural conception-children and from IVF-children.

Notwithstanding the above, current studies are not conclusive on whether the epigenetic disorders associated with ART are attributable to the ART protocol itself or the infertility background of couples. Three possible interpretations

may account for this: (1) First, in the ART procedure, the in vitro manipulation (such as in vitro embryo culture and transfer) overlaps with widespread epigenetic reprogramming [18], and this may influence the epigenetic modification of the embryo; (2) Second, the induction of superovulation may interfere with oocytes epigenetic establishment by changing the development timeline, recruiting low-quality oocytes or influencing epigenetic regulatory enzymes [19, 20]. Based on investigations on super ovulated women and mice, Sato et al. reported that [21] superovulation can lead to the production of oocytes without the correct primary imprint in both humans and mice; (3) And last but not least, the genetic background of the couples' self-sterility may also contribute to the genetic and epigenetic abnormalities in the offspring. There is no gainsaying the fact that most patients undergoing ART are typically of low fertility, advanced age, with a history of recurrent miscarriages, and involving male-factor infertility (such as azoospermia, asthenozoospermia, oligozoospermia, and teratozoospermia), either of which factors may contribute to abnormalities in fetal and neonatal development. Kobayashi et al. [22] also reported that the greater prevalence of imprinting disorders in ART children did not originate from the ART process alone, and a significant proportion of these epigenetic alterations pre-existed in the father's genetic line. Moreover, it is currently well recognized that no one procedure is fully/solely responsible for epigenetic changes after ART. Each of these factors has the potential to influence the establishment and maintenance of epigenetic modifications and affect placentation and fetal development.

2.2 The epigenome changes in the ART placenta

The placenta is a multifunctional organ at the maternal-fetal interface, with a critical role in maternal-fetal communication, such as maternal-fetal immune responses, nutrition and metabolism. The placenta is also a barrier organ to protect the fetus from invasion by pathogens [23]. Further, the placenta may regulate the development of fetal brain, heart, bones, kidneys, and other organs and tissues [24]. Hence, it is no surprise that placental dysplasia is known to cause adverse perinatal outcomes and long-term risks in fetal health, such as adult metabolic syndrome, neurodevelopmental disabilities and tumors [25, 26]. Notably, the placenta originates in the trophoctoderm (an outer layer of embryos in blastocyst stage) and therefore shows more sensitive response (e.g., epigenetic regulatory changes) to environmental influences and the non-physiologic interventions during ART procedure [27]. Animal studies have revealed that the in vitro culture and later transfer of embryos contributes to abnormal placenta development [28, 29]. Meanwhile, observational studies on humans have similarly revealed ART is associated with increased rates of placental abnormalities, such as adherent placentation and abnormal umbilical cord insertion [30, 31]. In a large sample observational study (n=536,567), researchers found ART-derived placenta both larger and heavier than those derived from natural conception [32]. Since the compromised function of the placenta is associated with abnormal fetus development, the assessment of placenta derived from ART-conception is helpful to gaining deeper insight into the influence of ART technologies on offspring.

Rhon-Calderon et al. [33] revealed that ART can influence the placenta by altering methylation status and the transcription of imprinted genes, which exert prominent roles in the placental function and fetal development [5]. St-Pierre et

al. [34] revealed that the DNA methylation levels of placental imprinted gene *IGF2* were correlated with newborn's weight, and the DNA methylation at the *IGF2/H19* genes may be a potential moderator of fetal normal growth. In a review article, Argyraki et al. [35] noted in summary that the imprinted genes *IGF2/H19*, *Paternally Expressed 10 (PEG10)* and *Mesoderm Specific Transcript (MEST)* in tissues such as placenta have extensive impacts on fetal growth and birth weight. The disruption of these imprinted genes is associated with pregnancy complications, metabolic disturbances, cognitive impairment, and cancers. Currently, imprint abnormalities in ART placenta have been revealed by both human studies and experimental animal models. Sakian et al. [36] investigated the transcriptional levels of imprinted genes, *H19* and *IGF2*, in human placental villi derived from IVF, ICSI, and natural conception using RT-qPCR, they found that *H19* and *IGF2* presented altered expression in IVF and ICSI placenta. They mentioned this might indicate a deletion of imprinting on paternal alleles. Wang et al. [37] investigated the transcription and DNA methylation levels of two other imprinted genes, *L3MBTL Histone Methyl-Lysine Binding Protein 1 (L3MBTL1)* and *PEG10*, in human placenta and umbilical cord blood from newborns. They found that *PEG10* showed both abnormal methylation status and transcription in both ART-placenta and umbilical cord blood from ART-offspring. While *L3MBTL1* only showed aberrant methylation and transcription in ART-placenta. In a mouse model, De Waal et al. [38, 39] found that ART procedures could increase placental epigenetic perturbations and morphological abnormalities by disturbing DNA methylation status of *H19/IGF2*, *PEG3*, *SNRPN* and *KCNQ1 Opposite Strand/Antisense Transcript 1 (KCNQ1OT1)* ICRs.

2.3 Transcriptome changes in aging oocytes

Despite the increasing popularity and improvements of ART, the live birth rate of IVF remains unsatisfactory. Advanced age-associated oocyte quality decline is one of the main causes for low IVF success rates. The most recent statistical report [40] indicates that, in Australia and New Zealand, for women less than 30 years old, the live birth rate was 40.4% (for autologous fresh cycles) and 33.9% (for autologous thaw cycles) per embryo transfer. While for the women aged more than 44 years, the live birth rate was 1.7% (for autologous fresh cycles) and 9.2% (for autologous thaw cycles) per embryo transfer. The low success rates of IVF mean that women undergo repeat IVF cycles, which may impose a heavy burden on women's mental and physical well-being. The high treatment costs will also place a significant burden on the health care system.

At the moment, the ICSI is the clear solution for impaired sperm quality, in this case, sperm could be microinjected into oocytes. However, oocyte aging and oocyte quality decline are still an unsolved problem. Fertilization of aged oocytes affects not only the embryo development but also the long-term health of offspring [41]. The investigation of the mechanisms underlying oocyte aging is helpful in developing targeted treatments to age-related oocyte quality decline as well as enhancing the success rates of ART technologies. Currently, several studies have investigated the impact of maternal age on human oocyte transcriptome via high-throughput technologies. However, the results from these studies were inconsistent. Two microarray studies reported that the transcriptome of oocytes at germinal vesicle (GV) stage shows no difference among women of different ages [42, 43]; while another single cell smart-seq2 study reported the expression of 596 genes in human GV oocyte is altered with

age [44]. In addition, based on microarray analysis, Grøndahl et al. [45] examined the genome-wide gene expression profiles of oocytes at metaphase II (MII) stage and found 342 differentially expressed genes between the young and old age groups (i.e., <36 years old vs. 37–39 years old) which may be involved in the sister chromatid separation, chromosome alignment, cell cycle regulation, oxidative stress and ubiquitination. Interestingly, contradicting the above finding, another study based on Affymetrix Human Transcriptome Arrays (HTA 2.0) [46] reported that the mRNA transcriptome of human MII oocytes remained stable across ages. Considering the sample sizes in the above studies were relatively small, multi-center studies with large sample sizes are still required to increase the persuasiveness of the results.

2.4 Introduction to epigenome and transcriptome

Epigenome refer to modulation of gene expression without changes of DNA sequence, it mainly includes (1) DNA methylation; (2) histone modifications (such as histone phosphorylation, acetylation, methylation, ubiquitylation, etc.); and (3) chromatin remodeling. DNA methylation alters chromatin architecture, DNA conformation and stability, and the way DNA interacts with proteins [47]. While histone modifications modulate gene expression by affecting the chromatin structure and chromatin accessibility to transcription factors [48]. For example, high enrichment of tri-methylated-histone-H3-lysine-4 (H3K4me3) characterizes open chromatin status and active transcription.

Epigenetic modifications are instrumental in cell development and are environmentally sensitive. The cells within an organism have the same genotype, but they can differ in phenotypes due to epigenetic heterogeneity which could result in differential gene expression [49]. Also, a person's susceptibility to dis-

ease is not only determined by the DNA inherited from parents but also determined by epigenetic mechanisms [49]. Epigenetic modification is sensitive to environmental influences and abnormal epigenetic modification has emerged as one of the important molecular pathogeneses for various diseases. Chromatin immunoprecipitation (ChIP) sequencing is a method that integrates high-throughput DNA sequencing technology and ChIP to detect nuclear protein-DNA interaction sites [50]. ChIP is a powerful tool for analyzing histone modification sites and transcription factor binding sites. For example, using H3K4me3 ChIP sequencing data can help to identify H3K4me3 enrichment levels at certain DNA sites, which is important because most H3K4me3 enrichment occurs at promoter regions (which are usually between the 3kb upstream of transcription start site (TSS) and the 500 bp downstream of TSS) [51]. Moreover, actively transcribed genes present high levels of H3K4me3 enrichment in promoter regions [52].

The transcriptome refers to all the RNA species transcribed within a cell or an ensemble of cells [53], such as messenger RNA (mRNA), transfer RNA (tRNA), ribosomal RNA (rRNA), and non-coding RNA (ncRNA). It is a mirror of genetic activity and is essential for transporting genetic information [54]. The central dogma of genetics reveals that genetic information unidirectionally flows from DNA to mRNA and then to proteins which finally determines cellular function and behavior. In this process, mRNA functions as a crucial bridge between DNA and protein. Transcriptome studies can help interpret the functional elements of the genome and reveal their molecular constituents [55]. Besides, transcriptome studies are also essential for understanding the biological mechanisms underlying human health and disease.

In recent years, the rapid developments in molecular biology have enabled rapid, high-throughput analysis, laying the groundwork for more in-depth transcriptomics studies. Current high throughput approaches mainly include microarrays (based on the hybridization detection) and RNA sequencing (based on massive parallel sequencing). Compared with traditional microarray hybridization, transcriptome sequencing could analyze global transcription profiles with no need to design probes to target the known sequences in advance. It is a powerful technology that allows comprehensive and in-depth looks into the transcriptome.

2.5 Aim of the study

To begin with, although ARTs have rapidly developed and have entered widespread use worldwide, more in-depth mechanism studies and large-scale life-long follow-up is still required to validate ART safety. Hence, the study aims to explore the epigenetic differences in placenta and offspring derived from natural conception, IVF and ICSI. The findings from this investigation might provide new insights into the safety and knowledge of ARTs.

Second, with the continuous advance of ART, success rates for ART are increasing but there is still much room for further improvement. Herein, we want to explore the transcriptomic changes during oocyte aging. Since oocyte aging is one of the main causes of ART failure, and remains an open question in the field of ART. It is believed that the results from this investigation will provide useful information for developing targeted therapies and improving ART success rates.

Taken together, it is hoped the present work could provide a reference for further refinement of ART.

3. Summary (English)

ARTs have been practiced clinically for over 40 years. But despite remarkable advances over the past four decades, two major problems remain outstanding and need to be explored in depth in the field of ARTs: (1) First, large sample-size and population-based studies have reported birth defects and perinatal complications associated with ART. To improve the safety and quality of ART, deeper insights are required into the molecular mechanisms behind this phenomenon; (2) Second, the overall success rates of ART are still not satisfactory. And impaired oocyte quality associated with advanced age is an important factor in low ART success rates. To improve the efficiency of ART practice, it is necessary to explore the molecular mechanisms underlying oocyte aging.

3.1 Epigenome changes in ART-derived placenta and offspring

The placenta is a critical component of the life support system of the fetus and could influence fetal development. Therefore, the present study investigated the epigenetic difference in placentae and newborns derived from IVF, ICSI, and natural conception. It was found that global H3K4me3 levels were reduced in ICSI-derived placentae, suggesting that ICSI technology may affect the placental epigenetic landscape. However, no significant difference was discovered in the global levels of H3K4me3 between the IVF and the natural conception groups. We also found the cord blood mononuclear cells from ICSI-offspring (but not IVF-offspring), especially ICSI-boy, presented more genes with altered H3K4me3 enrichment levels compared with those from natural conceived children. Besides, the present study identified Polr2A as a novel regulator of

H3K4me3. It was also found that oxygen tension can impact H3K4me3 enrichment, highlighting the importance of proper oxygen conditions during ART practice. Based on the above investigations, it is possible that H3K4me3 may act as a potential marker for assessing ART influences and this deserves further investigation.

3.2 Transcriptome changes in aging oocyte

Aging is the leading cause for impaired oocyte quality, which can further contribute to ART failure. We compared the transcriptomes of oocytes from young and old age groups and identified hundreds of genes with significant changes in transcript levels during oocyte aging. Functional enrichment analysis revealed these genes were enriched during DNA replication, cellular metabolism, and histone modifications. Notably, among these genes, the expression of *FAM111 Trypsin Like Peptidase A (FAM111A)* presented robust correlations with age in different datasets and analytical methods. *FAM111A* may also be involved in the regulation of cell cycle and chromosome segregation. As far as is known, neither another such study nor similar results have been reported. These findings could advance the understanding of the mechanisms behind oocyte aging, and potentially support the development of targeted treatments to age-related decline in oocyte quality.

Collectively, based on the comparison of epigenome in placentae and offspring derived from IVF, ICSI, and natural conception, the present study found that: (1) the placentae and newborn cord blood from ICSI, but not IVF group displayed altered H3K4me3 levels; (2) ICSI-boys presented more genes with altered H3K4me3 enrichment compared with ICSI-girls; and (3) H3K4me3 might be a promising biomarker for evaluating ART influence. On the other hand,

through exploring transcriptomic alterations during human oocyte aging, it found: (1) hundreds of genes underwent significant transcriptional changes during oocyte aging. (2) Among these age-related genes, *FAM111A* has potential as a novel molecular marker for oocyte aging. All the findings above could provide a reference for potential therapeutic targets and help improve the safety, quality, and efficiency of ART practice.

4. Zusammenfassung (Deutsch)

ARTs werden seit über 40 Jahren klinisch praktiziert. Trotz bemerkenswerter Fortschritte in den letzten 40 Jahren gibt es immer noch zwei große Probleme auf dem Gebiet von ARTs, die noch weiter erforscht werden müssen: (1) Erstens haben große Stichproben und bevölkerungsbezogene Studien über Geburtsfehler und perinatale Komplikationen im Zusammenhang mit ART berichtet. Um die Sicherheit und Qualität von ART zu verbessern, ist ein tieferer Einblick in die molekularen Mechanismen hinter diesem Phänomen erforderlich. (2) Zweitens ist die Gesamterfolgsquote der ART immer noch nicht zufriedenstellend. Die mit fortgeschrittenem Alter einhergehende verminderte Eizellenqualität ist ein wichtiger Faktor für die geringe Erfolgsquote der ART. Um die Effizienz der ART-Praxis zu verbessern, ist es notwendig, die molekularen Mechanismen der Eizellalterung zu erforschen.

4.1 Epigenetische Veränderungen in ART-abgeleiteten Plazenta und Nachkommen

Die Plazenta ist ein wichtiger Bestandteil des Lebenserhaltungssystems des Fötus und könnte die fötale Entwicklung beeinflussen. Wir untersuchten die epigenetischen Unterschiede in Plazenta und Neugeborenen aus IVF, ICSI und natürlicher Empfängnis. Wir haben festgestellt, dass die globalen H3K4me3-Spiegel in der ICSI-Plazenta reduziert waren, was darauf hindeutet, dass die ICSI-Technologie die epigenetische Landschaft der Plazenta beeinflussen könnte. Die globalen H3K4me3-Konzentrationen zeigten jedoch keinen signifikanten Unterschied zwischen IVF-Plazenta und Plazenta aus natürlicher

Empfängnis. Wir haben auch festgestellt, dass die mononukleären Zellen des Nabelschnurblutes von ICSI-Nachkommen (aber nicht von IVF-Nachkommen), insbesondere von ICSI-Jungen, mehr Gene mit veränderten H3K4me3-Anreicherungsgraden aufwiesen als die von Kindern mit natürlicher Empfängnis. Außerdem identifizierte unsere Studie Polr2A als einen neuartigen Regulator von H3K4me3. Wir haben noch festgestellt, dass die Sauerstoffspannung die H3K4me3-Anreicherung beeinflussen kann, was die Bedeutung einer angemessenen Sauerstoffversorgung in der ART-Praxis unterstreicht. Auf der Grundlage der obigen Untersuchungen ist es möglich, dass H3K4me3 ein potenzieller Marker für die Bewertung der Wirkungen von ART sein könnte und weitere Untersuchungen verdient.

4.2 Transkriptomischen Veränderungen in alternden Eizellen

Das Altern ist die Hauptursache für die Beeinträchtigung der Eizellenqualität, was weiter zum ART-Fehler führen kann. Wir haben das Transkriptom von Eizellen junger und alter Gruppen verglichen und Hunderte von Genen identifiziert, deren Transkriptionspiegel sich während der Alterung der Eizellen signifikant verändert. Die funktionelle Anreicherungsanalyse, dass solche Gene in den Bereichen DNA-Replikation, Zellstoffwechsel und Histonmodifikationen angereichert sind. Bemerkenswert ist, dass unter diesen Genen die Expression von *FAM111 Trypsin-ähnlichen Peptidase A (FAM111A)* in verschiedenen Datensätzen und Analysemethoden hohe Korrelationen mit dem Alter aufweist. *FAM111A* könnte an der Regulierung des Zellzyklus und der Chromosomensegregation beteiligt sein. Soweit bekannt, wurden weder eine weitere derartige Studie noch ähnliche Ergebnisse berichtet. Diese Ergebnisse könnten unser Verständnis der Mechanismen hinter der Alterung von Eizellen

wecken und möglicherweise die Entwicklung gezielter Krebstherapien gegen die altersbedingte Verschlechterung der Eizellenqualität unterstützen.

Insgesamt haben wir durch den Vergleich des Epigenoms in der Plazenta und in den Nachkommen aus IVF, ICSI und natürlicher Empfängnis festgestellt: (1) Die Plazenta und das neugeborene Nabelschnurblut der ICSI-Gruppe wiesen veränderte H3K4me3-Spiegel auf, während sich die in der IVF-Gruppe nicht verändert haben; (2) Im Vergleich zu ICSI-Mädchen wiesen ICSI-Jungen mehr Gene mit veränderter H3K4me3-Anreicherung auf; (3) H3K4me3 könnte ein vielversprechender Biomarker für die Bewertung der Wirkungen von ART sein. Andererseits haben wir bei der Untersuchung der transkriptomischen Veränderungen während der Alterung menschlicher Eizellen festgestellt: (1) Hunderte von Genen erfuhren während der Alterung von Eizellen signifikante transkriptionellen Veränderungen; (2) Unter diesen altersbedingten Genen hat *FAM111A* das Potenzial als neuartiger molekularer Marker für die Alterung von Eizellen. Alle oben genannten Erkenntnisse könnten als Referenz für potenzielle therapeutische Ziele dienen und dazu beitragen, die Sicherheit, Qualität und Effizienz der ART-Praxis zu verbessern.

5. Paper I



International Journal of
Molecular Sciences



Article

Comparison of Histone H3K4me3 between IVF and ICSI Technologies and between Boy and Girl Offspring

Huixia Yang ¹, Zhi Ma ¹, Lin Peng ¹, Christina Kuhn ^{1,2}, Martina Rahmeh ¹, Sven Mahner ¹, Udo Jeschke ^{1,2,*} and Viktoria von Schönfeldt ¹

¹ Department of Obstetrics and Gynecology, University Hospital, LMU Munich, 80337 Munich, Germany; huixia.yang@med.uni-muenchen.de (H.Y.); zhi.ma@med.uni-muenchen.de (Z.M.); lin.peng@med.uni-muenchen.de (L.P.); christina.kuhn@uk-augsburg.de (C.K.); martina.rahmeh@med.uni-muenchen.de (M.R.); sven.mahner@med.uni-muenchen.de (S.M.); viktoria.schoenfeldt@med.uni-muenchen.de (V.v.S.)

² Department of Obstetrics and Gynecology, University Hospital Augsburg, 86156 Augsburg, Germany

* Correspondence: udo.jeschke@med.uni-muenchen.de; Tel.: +49-821-400-165505

Abstract: Epigenetics play a vital role in early embryo development. Offspring conceived via assisted reproductive technologies (ARTs) have a three times higher risk of epigenetic diseases than naturally conceived children. However, investigations into ART-associated placental histone modifications or sex-stratified analyses of ART-associated histone modifications remain limited. In the current study, we carried out immunohistochemistry, chip-sequence analysis, and a series of in vitro experiments. Our results demonstrated that placentas from intra-cytoplasmic sperm injection (ICSI), but not in vitro fertilization (IVF), showed global tri-methylated-histone-H3-lysine-4 (H3K4me3) alteration compared to those from natural conception. However, for acetylated-histone-H3-lysine-9 (H3K9ac) and acetylated-histone-H3-lysine-27 (H3K27ac), no significant differences between groups could be found. Further, sex-stratified analysis found that, compared with the same-gender newborn cord blood mononuclear cell (CBMC) from natural conceptions, CBMC from ICSI-boys presented more genes with differentially enriched H3K4me3 ($n = 198$) than those from ICSI-girls ($n = 79$), IVF-girls ($n = 5$), and IVF-boys ($n = 2$). We also found that varying oxygen conditions, RNA polymerase II subunit A (Polr2A), and lysine demethylase 5A (KDM5A) regulated H3K4me3. These findings revealed a difference between IVF and ICSI and a difference between boys and girls in H3K4me3 modification, providing greater insight into ART-associated epigenetic alteration.

Keywords: assisted reproductive technologies; ICSI; IVF; H3K4me3; placenta; umbilical cord blood; imprint; oxygen; Polr2A; KDM5A



Citation: Yang, H.; Ma, Z.; Peng, L.; Kuhn, C.; Rahmeh, M.; Mahner, S.; Jeschke, U.; von Schönfeldt, V. Comparison of Histone H3K4me3 between IVF and ICSI Technologies and between Boy and Girl Offspring. *Int. J. Mol. Sci.* **2021**, *22*, 8574. <https://doi.org/10.3390/ijms22168574>

Academic Editor: Maurizio Battino

Received: 23 July 2021

Accepted: 6 August 2021

Published: 9 August 2021

Publisher's Note: MDPI stays neutral with regard to jurisdictional claims in published maps and institutional affiliations.



Copyright: © 2021 by the authors. Licensee MDPI, Basel, Switzerland. This article is an open access article distributed under the terms and conditions of the Creative Commons Attribution (CC BY) license (<https://creativecommons.org/licenses/by/4.0/>).

1. Introduction

Assisted reproductive technologies (ARTs) are involved at a critical window of embryo development, overlapping with extensive epigenetic reprogramming [1]. Epigenetic reprogramming plays a vital role in embryo development, with the possibility of being influenced by environmental exposure [2]. Studies in mice revealed that ARTs altered the cardiovascular phenotype via epigenetic alterations under sub-optimal culturing conditions [3–5]. A retrospective study based on a congenital mal-formations registry in France revealed that ART-conceived offspring have a three times higher risk of rare imprinting disorders associated with epigenetic dysregulation than naturally conceived children [6]. Epigenetic syndromes, such as Beckwith–Wiedemann syndrome (BWS), Silver–Russell syndrome (SRS), Prader–Willi syndrome (PWS), and Angelman syndrome (AS), have been observed in ART-offspring [6]. A meta-analysis of 18 studies concluded that children conceived through in vitro fertilization (IVF) and intracytoplasmic sperm injection (ICSI) have an increasing risk of imprinting disorders [7]. Placentas from ART children also presented altered DNA methylation compared with those from natural conception [8].

Interestingly, boys conceived using ART have been revealed to be more susceptible to ART-treatment-associated global DNA dys-methylation [8]. However, the factors contributing to the differences observed in ART children are complex. The infertility background of ART-parents [9], in vitro manipulation of embryo [10], and gonadotropin stimulation [11] are possible causes for epigenetic alterations.

As important epigenetic components, histone modifications play crucial roles in responses to developmental and environmental changes [12]. Tri-methylated histone H3 lysine-4 (H3K4me3) is a common histone H3 methylated form and a marker of active transcription, which is associated with open chromatin and stable up-regulation of the gene expression downstream of H3K4me3 promoter regions [13]. It is highly enriched in promoter regions [14] and involved in mammalian embryo development [15]. Acetylated histone H3 lysine-9 (H3K9ac) and acetylated histone H3 lysine-27 (H3K27ac) are common histone H3 acetylated forms associated with open chromatin and active gene transcription. They are enriched in active gene-regulatory regions, such as promoters and enhancers [16–18], and involved in prenatal intrauterine programming [16,17]. The placenta is a multifunctional organ essential for fetal development and survival [19]. It remains unclear whether global levels of these histone modifications show differences in placentas between natural conception and ARTs.

Oxygen tension is a primary environmental factor influencing epigenetic modifications of the in vitro embryo [20]. ART laboratories have been culturing pre-implantation gametes/embryos under atmospheric O₂ tension (20%), low O₂ tension (5%, similar to physiologic O₂ tensions in human fallopian tubes and uterus), and ultra-low O₂ tension (close or less than 5%) [21]. Placentas derived from in vitro 20% oxygen culture conditions showed a more significant difference in LINE1 methylation than those from in vivo conceptions, while placentas from in vitro 5%-oxygen-culture condition did not show significant differences [8]. A Cochrane review meta-analysis concluded that, compared with atmospheric O₂ tension, embryos cultured in low O₂ tension (5%) were better developed, bringing about higher probabilities of IVF/ICSI success, ongoing clinical pregnancy, live birth, and the birth of healthier offspring [22]. Nevertheless, the mechanisms by which low-oxygen culture improve the development of the in vitro embryo are not fully clarified. It has been revealed that high-oxygen culture perturbed gene expression, metabolism, and morphology in embryos [21]. However, further studies are needed to provide detailed data on the effects of low-oxygen culture during ARTs. In addition, despite the improvement in the O₂ tension of gametes/embryos culture systems, it is inevitable that ART practices are accompanied by the fluctuation of O₂ tensions [23]. The impact of fluctuating O₂ tensions on histone modification has been seldom studied.

Given the available evidence, we propose two hypotheses. The first hypothesis is that histone modifications might show up as differences in comparison between natural conception and ARTs, also in comparisons between ART-boys and ART-girls. The second is that varying oxygen conditions might influence histone modifications. We aim to test these two hypotheses and try to explore the potential regulators of histone modification.

2. Results

2.1. Global Levels of H3K4me3 Are Reduced in Placentas from Intracytoplasmic Sperm Injection (ICSI) Than Those from Natural Conception

Figure 1 presents a flowchart of the study design. Firstly, we performed immunohistochemistry (IHC) staining and IRS evaluation for H3K4me3, H3K9ac, and H3K27ac enrichment in placental tissues from natural conception, IVF, and ICSI groups. Supplementary Table S3 shows the clinical characteristics of three groups. H3K4me3, H3K9ac, and H3K27ac were immunolocalized to the syncytium, fetal endothelium, and decidua. Global H3K4me3 was more significantly reduced in placental syncytium ($p = 0.020$) and fetal endothelium ($p = 0.018$) from ICSI group than those from natural conception group (Figure 2). H3K4me3 showed no significant difference between natural conception and IVF groups ($p > 0.05$, Figure 2). H3K9ac or H3K27ac levels showed no significant difference between groups ($p > 0.05$).

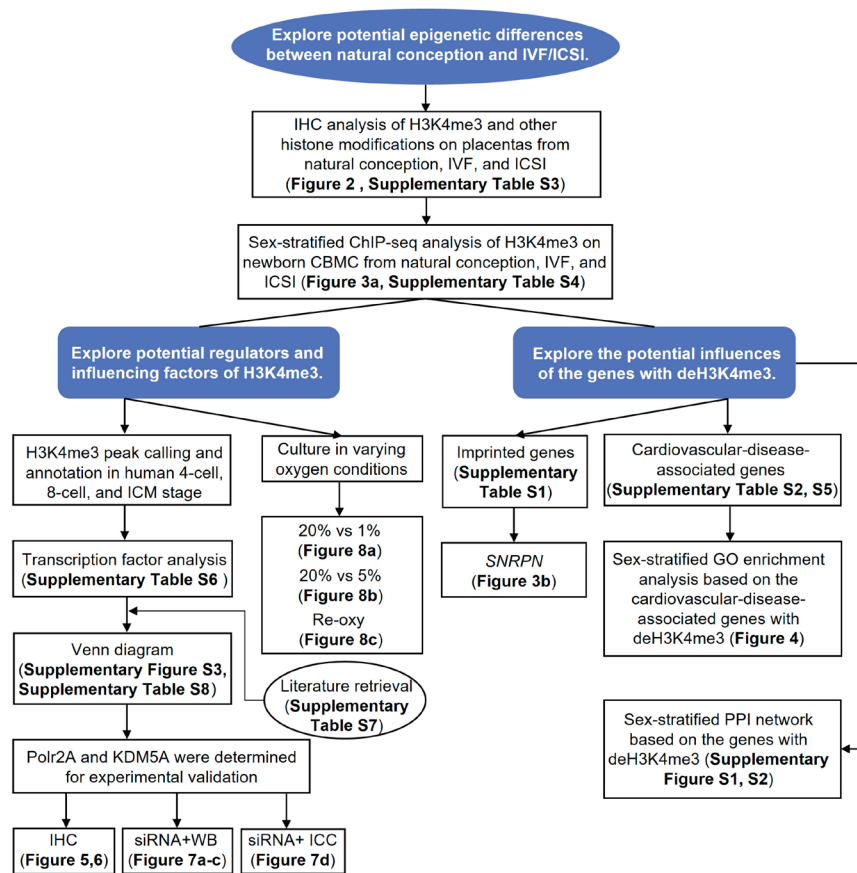


Figure 1. Flowchart of the study. IVF/ICSI, in vitro fertilization/intracytoplasmic sperm injection; IHC, immunohistochemistry; H3K4me3, tri-methylated histone H3 lysine-4; ChIP-seq, ChIP-sequence; CBMC, cord blood mononuclear cell; deH3K4me3, differentially enriched H3K4me3; ICM, inner cell mass; Polr2A, RNA polymerase II subunit A; KDM5A, lysine demethylase 5A; siRNA, small interfering RNA; WB, western blot; ICC, immunocytochemistry; 'Re-oxy' referred to intermittent hyperoxia exposure (5% O₂ 8 h + 20% O₂ 16 h + 5% O₂ 8 h); SNRPN, *small nuclear ribonucleoprotein polypeptide N*; GO, gene ontology; PPI, protein-protein interaction.

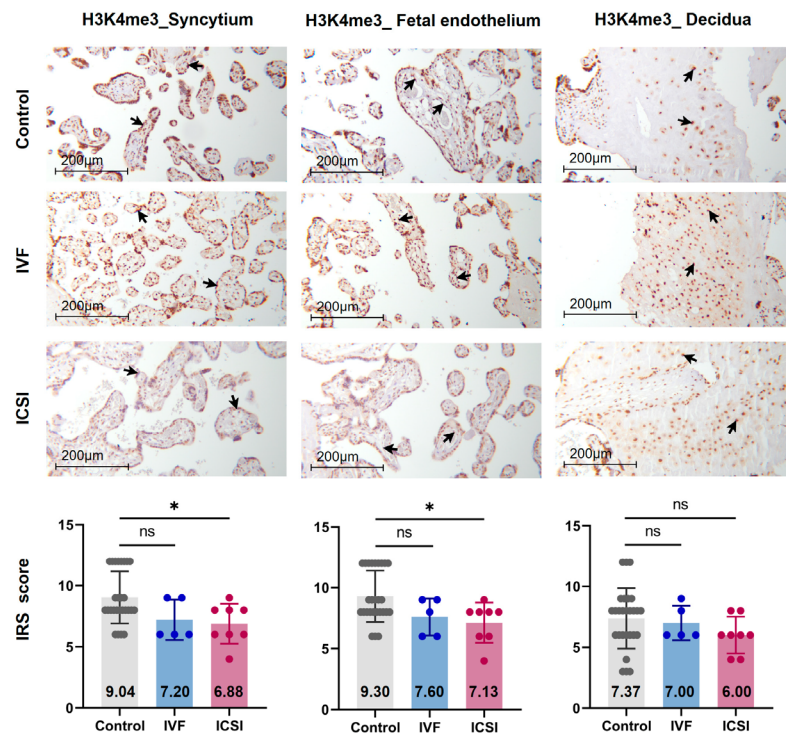


Figure 2. Global H3K4me3 was reduced in ICSI-derived placentas. Compared with natural conception placentas, ICSI placentas showed lower levels of H3K4me3 in syncytium and fetal endothelium, while IVF placentas showed no significant difference. Boxplots showing the IRS distribution among natural conception ($n = 27$), IVF ($n = 5$), ICSI ($n = 8$) groups along with significance levels indicated as p -value of the Mann-Whitney U -test. IRS = staining intensity \times percentage of positive cells. Data were reported as mean \pm SD. The arrows in the first, second, and third columns respectively pointed towards syncytial trophoblast cells, foetal endothelial cells and extravillous trophoblast cells. The numbers inside the columns represented the mean value of the corresponding IRS. IRS, immunoreactivity score; ns, non-significant. * $p < 0.05$.

2.2. The ICSI-Boys Present More Genes with Differentially Enriched H3K4me3 (deH3K4me3) Than In Vitro Fertilization (IVF)-Boys, ICSI-Girls, and IVF-Girls

When compared with the cord blood mononuclear cell (CBMC) from same-gender naturally-conceived-children, the CBMC from ICSI-boys presented more genes with differentially enriched H3K4me3 (deH3K4me3) ($n = 198$, $|\log \text{fold change (FC)}| > 1$ and false discovery rate (FDR) < 0.05) than those from ICSI-girls ($n = 79$, $|\log \text{FC}| > 1$ and FDR < 0.05), IVF-girls ($n = 5$, $|\log \text{FC}| > 1$ and FDR < 0.05) and IVF-boys ($n = 2$, $|\log \text{FC}| > 1$ and FDR < 0.05) (Figure 3a). Detailed reports of the genes with deH3K4me3 are available in the Supplementary Table S4. Protein–protein interaction (PPI) networks of the genes with deH3K4me3 from ICSI-boys and ICSI-girls are shown in Supplementary Figures S1 and S2. After overlapping the cardiovascular-disease-associated genes/imprinted genes with the genes with deH3K4me3, we found the ICSI-boys also presented more cardiovascular-disease-associated genes with deH3K4me3 ($n = 24$) than ICSI-girls ($n = 12$), while IVF-girls ($n = 0$) and IVF-boys ($n = 0$) did not show any cardiovascular-disease-associated genes with deH3K4me3. The overlapping gene list is available in Supplementary Table S5.

Moreover, ICSI-boys showed three imprinted genes with deH3K4me3 (i.e., *Small Nuclear Ribonucleoprotein Polypeptide N (SNRPN)*, *ZFP90 Zinc Finger Protein (ZFP90)*, and *DiGeorge Syndrome Critical Region Gene 6 (DGCR6)*) and ICSI-girls showed one imprinted gene with deH3K4me3 (i.e., *HNF1 Homeobox A (HNF1A)*). The H3K4me3 enrichment of imprinted gene *SNRPN* from naturally conceived-boys, IVF-boys, and ICSI-boys is shown in Figure 3b.

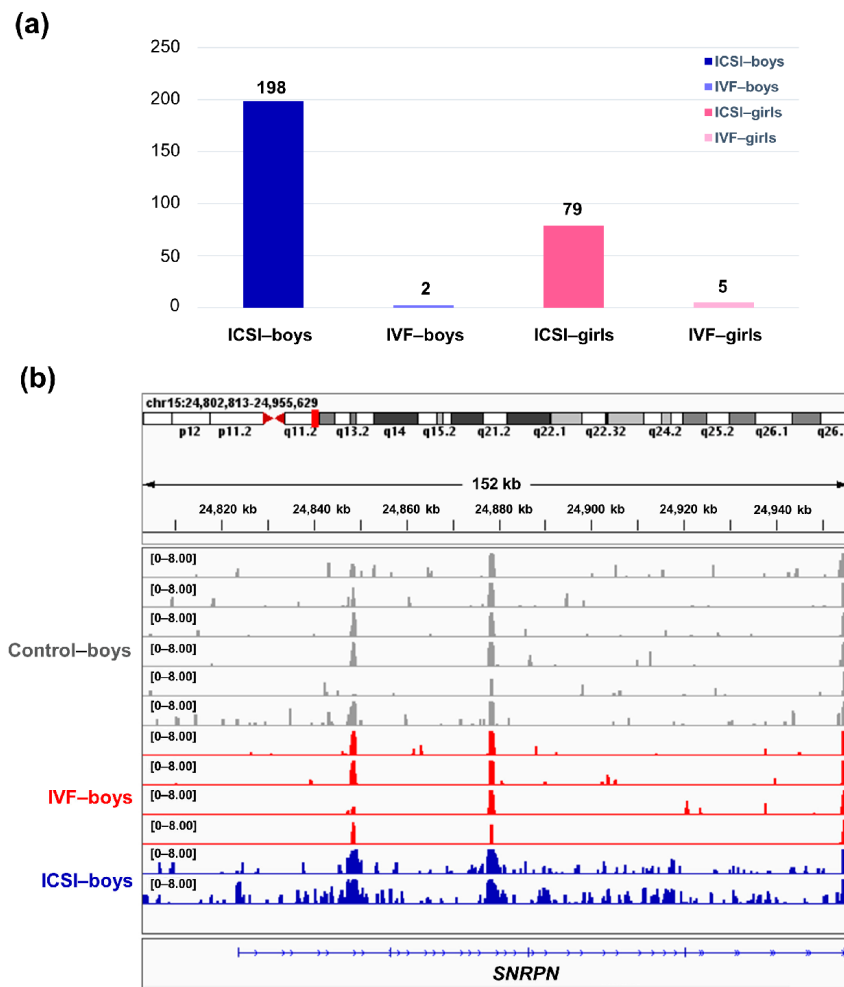


Figure 3. The ICSI-boys presented more genes with deH3K4me3 than IVF-boys, ICSI-girls, and IVF-girls. (a) The bar chart showed the comparison results of each gene promoter H3K4me3 read counts between natural conception-boys ($n = 6$) vs. ICSI-boys ($n = 2$), natural conception-boys ($n = 6$) vs. IVF-boys ($n = 4$), natural conception-girls ($n = 6$) vs. ICSI-girls ($n = 4$), and natural conception-girls ($n = 6$) vs. IVF-girls ($n = 4$). The comparison was performed via R package ‘edgeR’.

above the columns were the numbers of genes with significant H3K4me3 alteration in promoter region ($|\log FC| > 1$ and $FDR < 0.05$). (b) Genome browser snapshots of H3K4me3 ChIP-seq data at SNRPN loci in naturally-conceived-boys, IVF-boys, and ICSI-boys. H3K4me3 data showed the \log_2 enrichment ratio between H3K4me3 ChIP and the input. The data range was set at 0–8.00. FC, fold change; FDR, false discovery rate.

2.3. The Cardiovascular-Disease-Associated Genes with deH3K4me3 from ICSI-Girls Are Enriched in the Functions Associated with Cardiac Development

Gene ontology (GO) enrichment analysis showed the cardiovascular disease-associated genes with deH3K4me3 from ICSI-girls were enriched in ‘cardiocyte differentiation’, ‘ventricular cardiac muscle cell development’, and ‘ventricular cardiac muscle cell differentiation’ terms (adjusted p -values < 0.05 , Figure 4a). The GO terms for the ICSI-boys were mainly included ‘mitochondrial respiratory chain complex assembly’, ‘regulation of monocyte chemotactic protein–1 production’, and ‘monocyte chemotactic protein–1 production’ (adjusted p -values < 0.05 , Figure 4b).

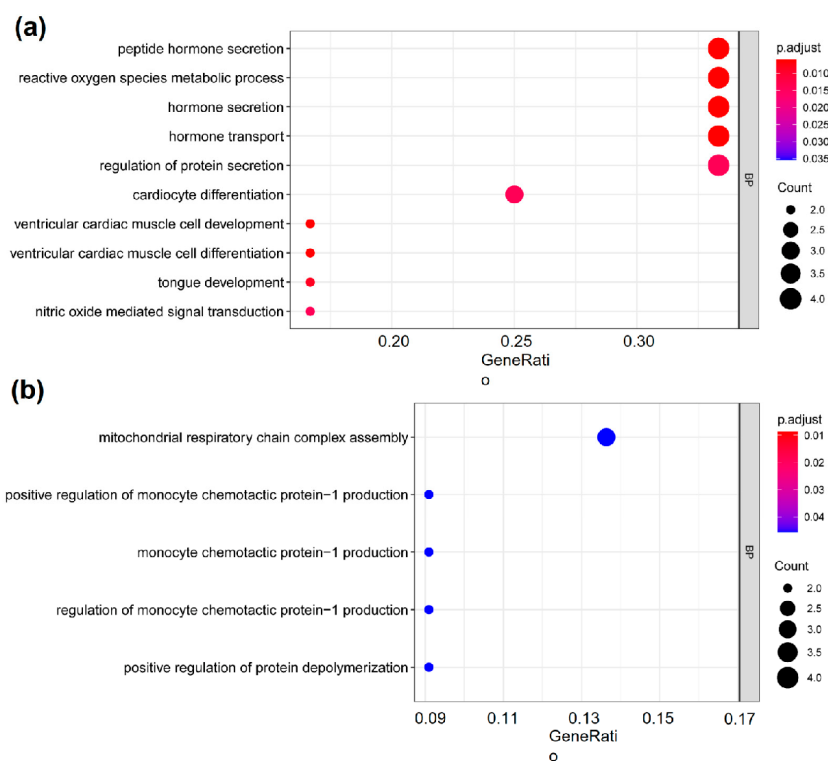


Figure 4. Genes with deH3K4me3 from ICSI-girls were enriched in ‘cardiocyte differentiation’ term. GO enrichment analysis of the genes with deH3K4me3 from (a) ICSI-girls and (b) ICSI-boys. The y-axis represented the significantly enriched terms (adjusted p -value < 0.05) in BP. The x-axis represented the GeneRatio (the ratio of the number of differential genes on the GO pathway to the total number of differential genes). The size of the dots represented the gene counts. The color gradient from red to blue meant the adjusted p -value from low to high. BP, biological process.

2.4. RNA Polymerase II Subunit A (Polr2A) and Lysine Demethylase 5A (KDM5A) Are the Regulators of H3K4me3

Through the TF analysis (results are available in Supplementary Table S6) by ‘RcisTarget’ package, literature retrieval on the potential regulators of H3K4me3 (results are available in Supplementary Table S7), and the overlapping results (Supplementary Figure S3, Supplementary Table S8) via ‘VennDiagrams’ package, we found RNA polymerase II subunit A (Polr2A), Transcription Factor AP-2 Gamma (TFAP2C), Kruppel Like Factor 15 (KLF15), etc. were involved in regulating genes enriched with H3K4me3 in four-cell, eight-cell, and inner cell mass (ICM) stages; lysine demethylase 5A (KDM5A), Sp3 Transcription Factor (SP3), Retinoic Acid Receptor Alpha (RARA), etc. were involved in regulating genes enriched with H3K4me3 in four-cell and ICM stages. Finally, Polr2A and KDM5A were selected for further experimental validations.

We conducted IHC staining and immune-reactive score (IRS) evaluation for Polr2A and KDM5A in placental tissues from natural conception, IVF, and ICSI. Polr2A and KDM5A were immunolocalized to the syncytium, fetal endothelium, and decidua (Figures 5 and 6). KDM5A expression was increased in the syncytium ($p < 0.001$), fetal endothelium ($p = 0.001$), and decidua ($p = 0.048$) of ICSI placentas than those in naturally-conceived-placentas. KDM5A expression showed no significant difference between natural conception and IVF groups ($p > 0.05$). Polr2A expression showed no significant difference between groups ($p > 0.05$).

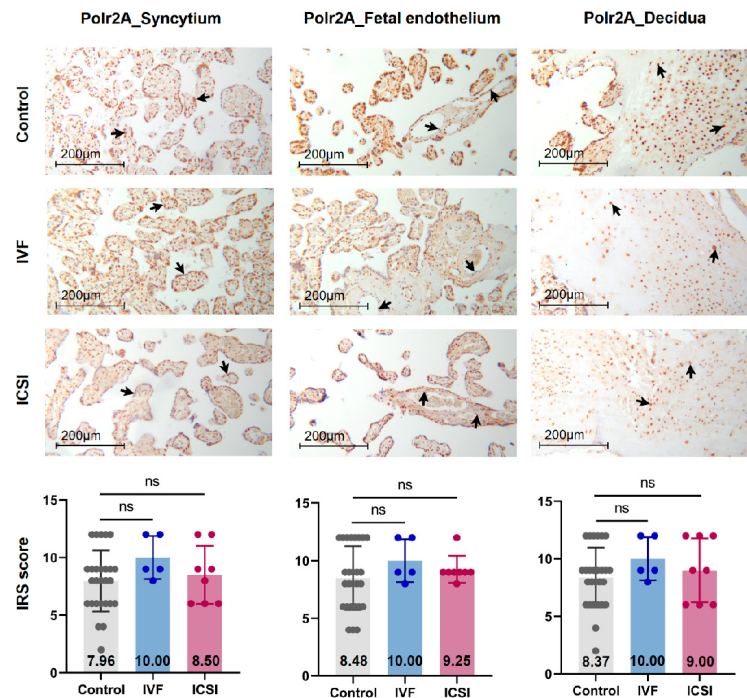


Figure 5. Polr2A expression showed no significant difference among natural conception, IVF, and ICSI-derived placentas. Polr2A levels showed no significant difference among groups. Boxplots showing the IRS distribution among natural

conception ($n = 27$), IVF ($n = 5$), ICSI ($n = 8$) groups along with significance levels indicated as p -value of the Mann-Whitney U -test. IRS = staining intensity \times percentage of positive cells. Data were reported as mean \pm SD. The arrows in the first, second, and third columns respectively pointed towards syncytial trophoblast cells, foetal endothelial cells and extravillous trophoblast cells. The numbers inside the columns represented the mean value of the corresponding IRS.

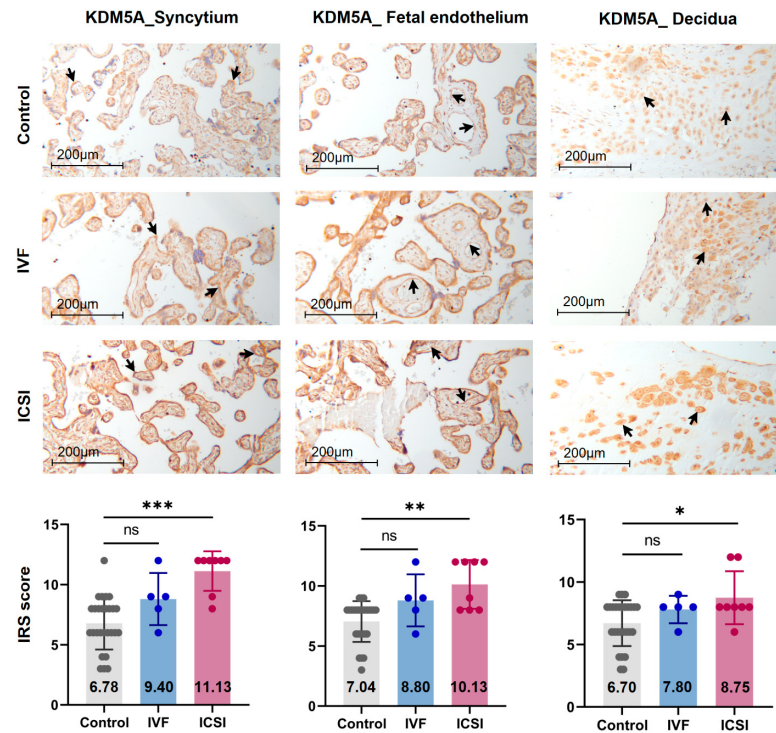


Figure 6. KDM5A expression was increased in ICSI-derived placentas. Compared with natural conception placentas, ICSI placentas showed higher levels of KDM5A in syncytium, fetal endothelium, and decidua, while IVF placentas showed no significant difference. Boxplots showing the IRS distribution among natural conception ($n = 27$), IVF ($n = 5$), ICSI ($n = 8$) groups along with significance levels indicated as p -value of the Mann-Whitney U -test. IRS = staining intensity \times percentage of positive cells. Data were reported as mean \pm SD. The arrows in the first, second, and third columns respectively pointed towards syncytial trophoblast cells, foetal endothelial cells and extravillous trophoblast cells. The numbers inside the columns represented the mean value of the corresponding IRS. * $p < 0.05$; ** $p < 0.01$; *** $p < 0.001$.

We transfected HTR-8/SVneo cells with siRNA targeting Polr2A (si-Polr2A), KDM5A (si-KDM5A), and non-targeting control siRNA (si-NT). Western blot analysis (Figure 7a–c) showed that H3K4me3 was significantly decreased ($p = 0.002$) after si-Polr2A transfection and significantly increased ($p = 0.043$) after si-KDM5A transfection. Immunocytochemistry (ICC) staining (Figure 7d) further verified this result. Compared with si-NT-cells, si-Polr2A-cells showed decreased levels of H3K4me3 ($p < 0.001$), si-KDM5A-cells showed increased levels of H3K4me3 ($p = 0.022$) at 72 h post-transfection.

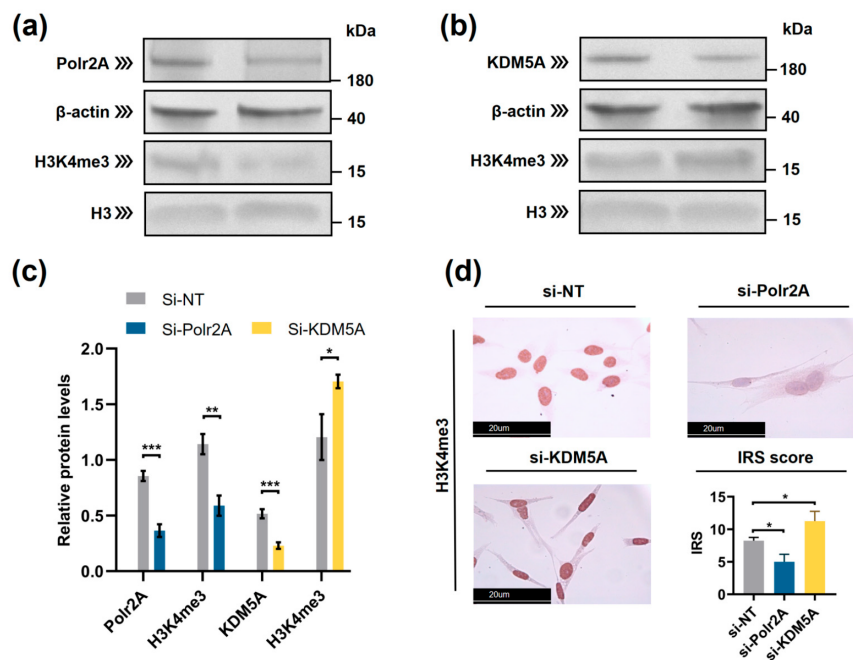


Figure 7. Polr2A and KDM5A regulated global levels of H3K4me3 in HTR-8/SVneo cells. (a–c) Western blot analysis and (d) immunocytochemistry showed that, compared with si-NT-cells, si-Polr2A-cells showed lower levels of H3K4me3 and si-KDM5A-cells showed higher levels of H3K4me3. In the boxplots, protein levels of Polr2A and KDM5A expressed relative to β -actin levels, protein levels of H3K4me3 expressed relative to histone H3 levels, IRS = staining intensity \times percentage of positive cells. Three independent experiments were performed. Data were reported as mean \pm SD. Independent samples *t*-test was used for statistical analysis. H3, Histone H3; si-NT, non-targeting control siRNA; si-Polr2A, siRNA targeting Polr2A; si-KDM5A, siRNA targeting KDM5A. * $p < 0.05$; ** $p < 0.01$; *** $p < 0.001$.

2.5. Varying Oxygen Conditions Regulate Protein Levels of Polr2A, H3K4me3, Hypoxia Inducible Factor 1 α (HIF 1 α) in HTR-8/SVneo Cells

Western blot analysis showed low-oxygen culture (1% O₂ (Figure 8a) and 5% O₂ (Figure 8b)) significantly increased protein levels of Polr2A, H3K4me3, and hypoxia inducible factor 1 α (HIF 1 α). The protein levels mostly peaked at 4 h post-culture. Protein levels of KDM5A only showed a significant increase at 4 h post-culture in 1% O₂ tension (Figure 8a).

Intermittent hyperoxia exposure resulted in significantly higher levels of H3K4me3 and HIF 1 α than persistent atmospheric oxygen culture ($p < 0.05$, Figure 8c) and significantly lower levels of H3K4me3 and HIF 1 α than persistent low-oxygen culture (5% O₂) ($p < 0.05$, Figure 8c).

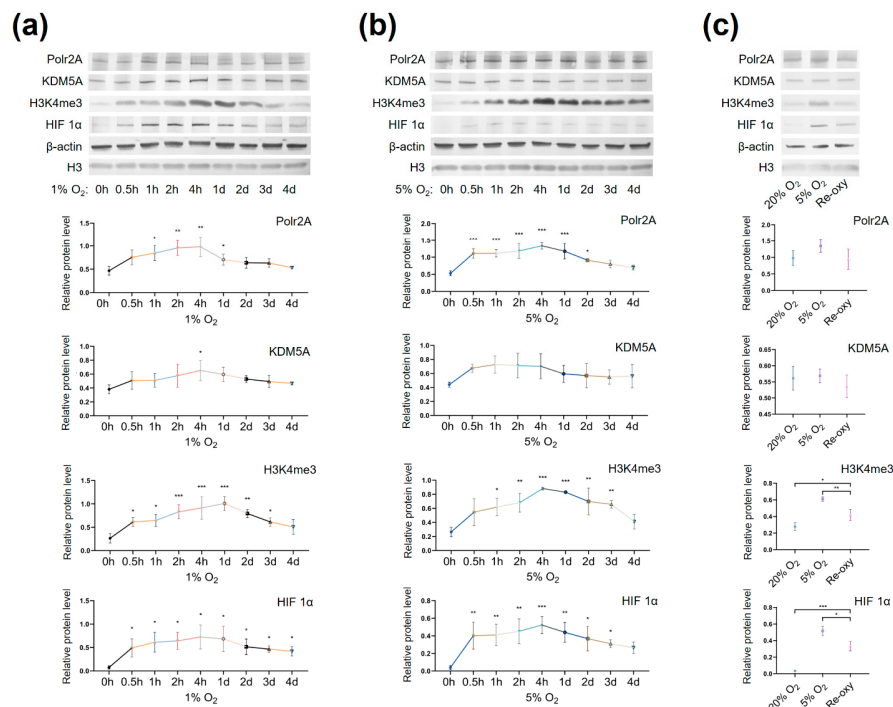


Figure 8. Protein levels of Polr2A, KDM5A, and H3K4me3 in varying oxygen conditions. After low-oxygen culture at 1% (a) and 5% O₂ (b), protein levels of Polr2A, H3K4me3, and HIF 1α were higher than atmospheric oxygen culture. After intermittent hyperoxia exposure (c), protein levels of H3K4me3 and HIF 1α were different from those after persistent atmospheric oxygen culture or persistent low-oxygen culture (5% O₂). In the boxplots, protein levels of Polr2A, KDM5A, and HIF 1α expressed relative to β-actin levels, protein levels of H3K4me3 expressed relative to histone H3 levels. Three independent experiments were performed. Data were reported as mean ± SD. One-way analysis of variance with Dunnett's post hoc test and independent samples *t*-test were used for statistical analysis. HIF 1α was used as the indicator for hypoxia. HIF 1α, hypoxia-inducible factor 1α. * $p < 0.05$; ** $p < 0.01$; *** $p < 0.001$.

3. Discussion

This study examined the levels of H3K4me3, H3K9ac, and H3K27ac in placentas from natural conception, IVF, and ICSI, and additionally compared the H3K4me3 read counts of each gene in CBMC from natural conception, IVF, and ICSI. Further, we investigated the potential regulatory mechanisms behind H3K4me3 alterations. Key findings were that, compared with naturally conceived placentas, placentas from ICSI but not IVF, showed global H3K4me3 alteration. Moreover, compared with CBMC from naturally conceived children, CBMC from ICSI-children, especially ICSI-boys, showed genes with deH3K4me3. Further, varying oxygen conditions, Polr2A, and KDM5A regulated H3K4me3.

Similar findings were recently reported by Chen and colleagues [24], who found that H3K4me3, but not H3K4me1, H3K27me3, or H3K27ac, showed differences in newborn CBMC from natural conception and ART groups. Herein, we found ICSI placentas showed lower levels of H3K4me3 than naturally conceived placentas. Meanwhile, for IVF placentas, H3K4me3, H3K9ac, or H3K27ac showed no significant difference in comparison

to the control group. Considering that IVF is a process of natural selection whereas ICSI manipulation is invasive, there is biologic plausibility to support our findings. Notably, H3K4me3 is a promising biomarker that could convey important information. A gain in H3K4me3 enrichment is associated with loss of DNA methylation, open chromatin, and active gene transcription [13,25]. Thus, it has been adopted as a marker to identify genes that were transcriptionally active [26]. Besides, H3K4me3 is the most affected histone modification in the in vitro culture system [27]. A previous study suggested that H3K4me3 may potentially serve as a marker for evaluating the influence of ARTs [24].

Our sex-stratified analysis revealed that, when comparing CBMC from same-gender naturally-conceived-children, ICSI-boys presented more genes with deH3K4me3 than ICSI-girls, while IVF-children showed a very tiny number of genes with deH3K4me3. GO enrichment analysis further revealed that cardiovascular-disease-associated genes with deH3K4me3 from ICSI-girls were enriched in the functions associated with cardiac development. A meta-analysis incorporating 4096 naturally-conceived-offspring and 2112 ART-offspring also found an increased risk of cardiovascular diseases among human ART-offspring [28]. Likewise, Ghosh and colleagues [8] revealed that ART boys were more susceptible to ART-treatment-associated global DNA dys-methylation. Another study also revealed that male offspring presented more robust responses and neurobehavior alterations to maternal inflammation [29]. One possible explanation is the sex-specific differences in the sensitivity to external exposure. However, further studies are encouraged to make an intensive study and elucidate the underlying mechanisms.

We also found three imprinted genes in ICSI-boys (i.e., *SNRPN*, *ZFP90*, and *DGCR6*) and one imprinted gene in ICSI-girls (i.e., *HNFLA*) presented deH3K4me3 at promoter. Likewise, Choux and colleagues [30] checked five kinds of histone modifications in placentas from natural conception and IVF/ICSI, found the permissive marker H3K4me2 enrichment at the differentially methylated regions of *H19/IGF2* and *KCNQ1OT1* was significantly higher in IVF/ICSI group than those in natural conception group, and revealed that the epigenetic changes of imprinted genes at birth might be an important developmental event caused by ART manipulations. Rivera and colleagues [31] found that even the most basic manipulation (i.e., embryo transfer) could contribute to the mis-expression of imprinted genes during post-implantation development. Meanwhile, the in vitro culture followed by embryo transfer could make the situation worse, specifically by increasing numbers of aberrant imprinted genes in mouse embryos, yolk sacs, and placentas, with even some fetuses exhibiting aberrant imprinted genes. The disruption of *SNRPN* has been revealed to play a role in AS and PWS, which are the major imprinting disorders in ART children [6,32].

We found that, after low-oxygen culture (1% and 5% O₂), global levels of H3K4me3 were significantly higher than those after atmospheric oxygen culture. Besides, after intermittent hyperoxia exposure, global H3K4me3 levels were significantly different from those after persistent atmospheric culture and low-oxygen culture. Our findings agree with previous studies [33–35] which have reported that, in low oxygen tensions (1% O₂ and less than 0.5% O₂), global levels of H3K4me3 increased in multiple human cell lines (e.g., HeLa cells, HFF cells, A549 cells, Beas-2B cells, and hADSC Cells). Intermittent hyperoxia exposure may also contribute to H3K4me3 alteration [36]. Further, we hypothesize that the oxygen tensions and intermittent hyperoxia exposure-associated H3K4me3 alteration in our cell culture system may have been due to the increased production of reactive oxygen species (ROS). It is known that higher O₂ tension and re-oxygenation are both accompanied by increased generation of ROS [37,38]. Unlike the in vivo system, culture conditions in vitro lack naturally effective antioxidant systems [39]. Excessive ROS produced in impaired cellular antioxidant systems may further contribute to redox imbalance [40], influencing redox-sensitive TFs and critical enzymes associated with histone modifications [39]. One previous study has also proposed that H3K4me3 is redox-regulated, and the ROS reagent H₂O₂ results in decreased levels of H3K4me3 [41]. Currently, in human embryo culturing systems, it is common to supplement antioxidants, yet how to maintain a prooxidant–antioxidant equilibrium still deserves further investigation.

Typically, enzymes that catalyze H3K4me3 include both histone lysine methyltransferases (known as 'writers') and demethylases (known as 'erasers'). These enzymes mediate the dynamic regulation of H3K4me3 [42]. Other proteins/molecules, such as Pygo2 [43], Polycomb group ring finger 6 (PCGF6) [44], and Interleukin-13 (IL-13) [45], have also been found to be involved in H3K4me3 regulation. In the present study, we found that Polr2A and KDM5A participated in regulating H3K4me3 in human HTR-8/SVneo cells. Polr2A (synonyms: Polr2, PolrA, and RPB1) is the largest subunit of RNA polymerase II (Pol II), and it plays a fundamental part in the enzymatic activity of Pol II [46]. A previous study revealed that in oxidative stress conditions, Polr2A could be regulated by pVHL and PHDs [46] (known as 'oxygen sensors' [47]). Treatment of 786-O cells with hydrogen peroxide (H₂O₂) resulted in a significant induction of phosphorylated Polr2A [46]. In addition, intermittent hypoxia and UV irradiation have also been shown to be able to induce Polr2A ubiquitylation and degradation [48,49]. As mentioned above, Polr2A is a fundamental part of Pol II. Moreover, a previous study revealed that H3K4me3-associated active interacting domains were mostly embedded in Pol II-associated transcriptional interacting domains [50]. However, our study provided the first evidence that Polr2A positively regulated H3K4me3 enrichment, revealing that Polr2A might play a role in promoting a more permissive chromatin conformation [51].

As is known, KDM5A (synonyms: JARID1A and RBP2) is a histone lysine demethylase (KDM) and described as an 'oxygen sensor' because KDM5A activity is oxygen-sensitive in various cellular systems [52]. In depleted oxygen conditions, the activity of histone lysine demethylases is inhibited, and as compensation, the expressions of histone lysine demethylases are commensurately increased [34]. A study of HepG2 hepatoma cells reported that mRNA and protein levels of lysine demethylase 5B (KDM5B) were higher following exposure to low and severely low oxygen tensions [53]. However, in another study (on Beas-2B cells), low-oxygen treatment was not found to cause any significant change of KDM5A in both mRNA and protein levels [35]. The variability of the findings in these studies may, however, reflect different experimental conditions and cell type specificities. Notably, the increased histone trimethylation under low oxygen tensions mainly resulted from attenuated catalytic activities of histone demethylases and not from altered abundances of histone demethylases [34]. KDM5A is able to catalyze the removal of all three methyl groups from H3K4 lysine residue and is essential for early embryo development [54]. Knockdown of KDM5A in HeLa cells is stated to contribute to the global increase of H3K4me3 [55]. Moreover, our knockdown experiment in HTR-8/SVneo cells further verified that KDM5A is a negative regulator of H3K4me3. In the IHC staining, KDM5A also showed an opposite expression trend compared to H3K4me3. Furthermore, in our TF analysis, the KDM5A was involved in regulating H3K4me3 in the four-cell and ICM stages, but not in the eight-cell stage. This may be due to the expression of KDMs being stage-specific during embryogenesis [56].

Limitations in the current study: (1) The current study only verifies the regulating effect of two H3K4me3 regulators via knock-down experiment, and over-expression experiments are thus necessary for future studies. It is also recommended to carry out co-immunoprecipitation (co-IP) to explore whether a direct interaction exists between Polr2A and H3K4me3. (2) Due to the limited sample size of the placental tissues, we did not perform a sex-stratified IHC analysis. However, considering the potential gender differences in epigenetics, it is recommended that a sex-stratified analysis be performed when the sample size is sufficient. (3) When we compared H3K4me3 read counts of each gene between the natural conception and ART groups, to ensure sufficient confidence, we defined 'genes with deH3K4me3' as $|\log FC| > 1$ and $FDR < 0.05$, and based on this condition, we obtained a limited number of genes with deH3K4me3 and a limited number of GO terms. In order to get more GO terms, relaxing the screening thresholds of 'genes with deH3K4me3' may be advisable. (4) Considering the ICSI is usually prepared for male oligospermia, asthenospermia, or abnormal fertilization in previous conventional IVE, the alteration of H3K4me3 in ICSI group may not only derive from ICSI technology

per ser, but also from the couple's infertility background. Sometimes, it is hard to make the natural conception group and ICSI group perfectly comparable, but it is necessary to minimize confounding variables. In addition, it would be advisable to record the clinical and genetic/epigenetic information of couples. At present, ART technology is only 43 years old, and a well-designed multi-center large-scale prospective study is still lacking for the technology. However, long-term follow-up is indeed necessary to evaluate the health of ART-offspring and clarify the safety of ART.

4. Materials and Methods

4.1. Ethics

The study was performed under the approval of the Ethics Committee of Medical Faculty, Ludwig Maximilians University Munich (NO.: 337-06). Each participant who joined in this study provided written informed consent.

4.2. Study Participants and Sample Collection

Term uncomplicated pregnancies were recruited in the Gynaecological and Obstetric Department of two LMU hospitals, Campus Innenstadt and Campus Großhadern, Germany. The study participants included three categories: IVF-conceived pregnancies ($n = 5$), ICSI-conceived pregnancies ($n = 8$), and spontaneously conceived pregnancies within one year after stopping contraceptive methods ($n = 27$). The exclusion criteria for this study were as follows: (1) preterm birth or still-birth; (2) twin or multi-fetal pregnancies; (3) pregnancy over 40 years old; (4) maternal neurological, cardiac or pulmonary disorders, HIV infections, hepatitis B/C infections, alcohol abuse, drug addiction, diabetes, hypertension, hyperthyroidism, Hashimoto's disease, other severe autoimmune diseases or metabolic syndromes; (5) fetal intrauterine infection, growth retardation, malformation, or other birth defects.

After vaginal delivery or cesarean section delivery, placental samples ($2 \times 2 \times 2 \text{ cm}^3$) containing amnion, villous, and decidua were taken from the central placental cotyledon with sufficient blood supply and embedded in paraffin blocks after 24-h fixation in a 4% buffered formalin solution.

4.3. Immunohistochemistry (IHC)

To explore the histone modification levels in placentas from natural conception and ARTs. Global H3K4me3, H3K9ac, and H3K27ac were compared via IHC on placental tissues. After pre-treatment of formalin-fixed, paraffin-embedded sections, placental tissues were incubated with primary antibodies for 16 h at 4 °C. The primary antibodies included rabbit anti-H3K4me3 (1:100; Abcam, Cambridge, MA, USA, Cat# ab8580; RRID: AB_306649), anti-H3K9ac (1:200, Abcam Cat# ab32129, RRID: AB_732920), anti-H3K27ac (1:2,000; Abcam, Cat# ab177178; RRID: AB_2828007), mouse anti-Polr2A (1:500, OriGene, Rockville, MD, USA, Cat# CF810050), rabbit anti-KDM5A (1:300, Thermo Fisher Scientific, Waltham, MA, USA, Cat# PA5-50741; RRID: AB_2636193). For detection, a horseradish peroxidase-coupled anti-mouse/rabbit polymer system (Zytomed Systems, Berlin, Germany, Cat# POLHRP-100) was used with DAB (Dako, Glostrup, Denmark, Cat# K3468) as the chromogen. The expression of primary antibodies was evaluated by two independent, blinded observers using semi-quantitative IRS [57]. IRS (range of 0 to 12) was obtained by multiplying the score of intensity (0 = no; 1 = weak; 2 = moderate; or 3 = strong staining) and that of the extent of positive cells (0 = none; 1 = 1–10%; 2 = 11–50%; 3 = 51–80%; 4 = 81–100%).

4.4. Sex-Stratified ChIP-Sequence Analysis

To further compare the sex-stratified H3K4me3 levels in newborn CBMC from natural conception and ARTs, H3K4me3 ChIP-sequenced data were taken from NCBI Gene Expression Omnibus (GEO, <http://www.ncbi.nlm.nih.gov/geo/> (accessed on 1 June 2021)) (accession number: GSE136849; GSM4082456–79, GSM4082482–3). A total of 26 ChIP samples from twin pregnancies were included for sex-stratified analysis: 6 samples from

naturally-conceived-boys, 4 samples from IVF-boys, 2 samples from ICSI-boys, 6 samples from naturally-conceived-girls, 4 samples from IVF-girls, and 4 samples from ICSI-girls. Firstly, the bigwig file was transferred to the 'bedGraph' file via 'bigWigToBedGraph' tool. Then, the read counts per promoter (the region between 3kb upstream to 500bp downstream of the transcription start site (TSS)) were determined via Bedtools (Version 2.29.0). H3K4me3 read counts of each gene between the natural conception and ART groups were compared via R package 'edgeR' (version 3.32.0). Genes with the $|\log FC| > 1$ and the $FDR < 0.05$ were selected as the genes with differentially enriched H3K4me3 (deH3K4me3) and annotated with ENTREZ Gene IDs via R package 'org.Hs.eg.db' (version 3.8.2).

The imprinted genes (Supplementary Information Table S1) were compiled from the Geneimprint database (<http://www.geneimprint.org/>, accessed on 1 June 2021) and the study of Petry and colleagues [58]. Then, the imprinted genes were annotated with ENTREZ Gene IDs via R package 'org.Hs.eg.db' (version 3.8.2). The imprinted genes, with their role in regulating fetal growth [59], have been investigated in studies on fetal health [58,60]. The overlapping results of the imprinted genes and the genes with deH3K4me3 were obtained via VLOOKUP functions in Microsoft Excel. H3K4me3 ChIP-seq signal of genes was visualized using Integrative Genomic Viewer (IGV, version 2.9.4, <http://www.broadinstitute.org/igv> (accessed on 1 June 2021)).

The cardiovascular disease-associated genes (Supplementary Table S2) were downloaded from RGD cardiovascular disease portal (<https://rgd.mcw.edu/rgdweb/portal/home.jsp?p=3>, accessed on 21 June 2021). Then, the cardiovascular disease-associated genes were annotated with ENTREZ Gene IDs via R package 'org.Hs.eg.db' (version 3.8.2). The overlapping results of the cardiovascular disease-associated genes and the genes with deH3K4me3 were obtained via VLOOKUP functions in Microsoft Excel.

4.5. Gene Ontology (GO) Analysis and Protein–Protein Interaction (PPI) Networks

To explore the effect of genes with deH3K4me3 on the cardiac development of children, we conducted GO enrichment analysis, with the cardiovascular disease-associated genes with deH3K4me3 as gene-list and with the whole cardiovascular disease-associated genes as background. GO analysis was carried out via R software 4.0.2 (Vienna, Austria) and R-package 'ClusterProfiler' (version 3.16.0) and the terms with an adjusted p -value < 0.05 were selected as significantly enriched GO term.

PPI networks of the genes with deH3K4me3 from ICSI-boys and ICSI-girls were constructed via STRING database (<https://string-db.org/> (accessed on 22 June 2021)), with a medium confidence score of 0.4 as the minimum required interaction score.

4.6. H3K4me3 Regulators Prediction

To find the potential regulators of H3K4me3 during early embryo development, H3K4me3 CUT&RUN data (accession number: GSE124718; from human pre-implantation embryos including 4-cell, 8-cell, and ICM stages) were downloaded from the GEO. Then, the downloaded files were converted into fastq files via 'fastq-dump' (version 2.8.2) from the SRA Toolkit (<https://github.com/ncbi/sratoolkit> (accessed on 6 March 2020)). Bowtie2 software 2.1.0 and MACS2 software 2.1.2 were adopted for mapping and peak-calling (4kb upstream to 4kb downstream of the TSS). R software 4.0.2 (Vienna, Austria) and R-package 'ChIPseeker' (version 1.14.1) were used to retrieve the nearest genes around the H3K4me3 peak and annotate the genomic features. Based on the above analysis, we obtained the genes that were enriched with H3K4me3 at promoter. The regulators of H3K4me3 were then predicted by R-package 'RcisTarget' (version 1.4.0) based on these genes. 'RcisTarget' is an R package that identifies the enriched transcription factor (TF) binding motifs and the upstream candidate TFs for a gene list. Motifs with a normalized enrichment score (NES) over 3.0 were retained. To determine the candidate regulators of H3K4me3 for experimental validation, literature retrieval was also conducted in NCBI-PubMed, Google Scholar, Web of Science, EMBASE, and Cochrane Library. Afterwards, a Venn diagram was

drawn to compare and identify the overlapping results from TF analysis and literature retrieval via R package 'VennDiagram' (version 1.6.20).

4.7. Cell Transfection Validation

Human trophoblast HTR-8/SVneo cells were purchased from the American Type Culture Collection (ATCC, Manassas, VA, USA, Cat# CRL-3271; RRID: CVCL_7162), which were cultured on 4-well chamber slides and a 4-well plate containing Opti-MEM Reduced Serum Media (Gibco, Grand Island, NY, USA) without antibiotics/antimycotics in a standard incubator (37 °C, 5% CO₂). siRNAs targeting Polr2A (Qiagen, Hilden, Germany, Cat# SI04354420) and KDM5A (Origene, Cat# SR304002B), and negative control siRNA (Qiagen, Cat# 1027280) were transfected into HTR-8/SVneo cells using Lipofectamine RNAiMAX transfection reagent (Invitrogen, Carlsbad, CA, USA, Cat# 2232175) as per the manufacturer's protocol. For transfection with siRNA targeting Polr2A, cells were transfected once, followed by 72 h of incubation at 37 °C. For transfection with siRNA targeting KDM5A, cells were transfected twice with siRNA in an interval of 24 h, followed by 48 h of incubation at 37 °C.

4.8. Immunocytochemistry (ICC)

ICC was used to study the global levels of H3K4me3 after siRNA transfection. Cells were fixed on slides and incubated with rabbit anti-H3K4me3 antibodies (1:500; Abcam, Cat# ab8580; RRID: AB_306649) for 16 h at 4 °C. HRP-coupled anti-mouse/rabbit polymer system (Zytomed Systems, Cat# POLHRP-100) was used for detection, with DAB (Dako, Cat# K3468) as the chromogen. The levels of H3K4me3 were evaluated by two independent, blinded observers using IRS [57].

4.9. Cell Culture in Varying Oxygen Conditions

Next, to investigate the influence of oxygen tensions on global levels of H3K4me3 and its regulators, we cultured HTR-8/SVneo cells in different oxygen conditions. Cells were spread evenly on plates containing RPMI Medium 1640 + GlutaMAX (Gibco) + 10% Fetal Bovine Serum (Gibco) without antibiotics/antimycotics and kept overnight in a standard incubator (37 °C, 5% CO₂). For low-oxygen culture, cells were placed in the tri-gas incubator (37 °C, 5% CO₂, 1% or 5% O₂, and N₂) with series of culture periods ranging from 0.5 h to 4 days. For atmospheric oxygen culture (negative controls), cells were continuously grown in a standard incubator. For intermittent hyperoxia exposure, cells were exposed to 5% O₂, 20% O₂, and 5% O₂ in sequence. A more detailed description of the low-oxygen culture and intermittent hyperoxia exposure is provided in the Supplementary Information.

4.10. Western Blots

Cells were washed and aliquoted into two tubes to prepare histone and total proteins. Histone proteins were extracted using a histone extraction kit (Abcam, Cat# ab113476) as per the manufacturer's instructions. Total proteins were obtained using radioimmunoprecipitation assay buffer (RIPA; Sigma-Aldrich, St Louis, MO, USA, Cat# R0278) containing protease inhibitor (Sigma-Aldrich, Cat# P8340). Twenty micrograms per well for total proteins and 10 µg/well for histone proteins were separated using SDS-PAGE and transferred to PVDF membranes (Roche Applied Science, Penzberg, Germany) for total proteins and nitrocellulose membranes (Li-COR Biosciences, Lincoln, NE, USA) for histone proteins. Membranes were incubated with primary antibodies, including rabbit anti-H3K4me3 (1:1000; Abcam, Cat# ab8580; RRID: AB_306649), mouse anti-Polr2A (1:500; Origene, Cat# CF810050), rabbit anti-KDM5A (1:500; Thermo Fisher Scientific, Cat# PA5-50741; RRID: AB_2636193), rabbit anti-HIF 1α (1:1000; Cell Signaling Technology, Danvers, MA, USA, Cat# 14179; RRID: AB_2622225), mouse anti-β-Actin (1:1000; Sigma-Aldrich, Cat# A5441; RRID: AB_476744), and rabbit anti-histone H3 (1:500; Cell Signaling Technology, Cat# 4499; RRID: AB_10544537) for 16 h at 4 °C and incubated with goat anti-rabbit (1:1000; Jackson ImmunoResearch Labs, West Grove, PA, USA, Cat# 111-055-144; RRID: AB_2337953)/goat

anti-mouse (1:1000; Jackson ImmunoResearch Labs, Cat# 115-055-062; RRID: AB_2338533) secondary antibodies for two hours at room temperature (around 22–25 °C). Final signals were detected using NBT/BCIP (Promega, Madison, WI, USA, Cat# S380C/S381C). Densitometry analysis was performed using Gel Doc XR + Imaging System with Quantity One Software (Bio-Rad Laboratories, Munich, Germany).

4.11. Sample Size Estimation for Immunohistochemistry

For IHC experiments, sample size was determined based on the IRS values of H3K4me3 from placental villi. According to the pre-test, the mean value of control, IVF, and ICSI groups was respectively 11.00 ($n = 3$), 7.00 ($n = 3$), and 6.67 ($n = 3$). The overall standard deviation (SD) was 2.49 ($n = 9$). ‘Multiple Comparisons of Treatments vs. a Control (Simulation)’ of PASS software 15.0 (Kaysville, UT, USA) was used for sample size estimation (input parameter: Type I error, $\alpha = 0.05$; power, $1 - \beta = 0.8$; the test1/test2/control sample proportion was set at 1:1:4). To reach sufficient statistical power (>0.8), the overall sample size > 26 was recommended.

4.12. Statistical Analysis

Statistical analyses were conducted via SPSS 26.0 (Chicago, IL, USA) and GraphPad Prism 8.4.3 (San Diego, CA, USA) software. Each assay was repeated in three independent experiments. Independent samples *t*-test, Mann–Whitney *U*-test, One-way analysis of variance (ANOVA) with Dunnett’s post hoc test, and Chi-square test were adopted for comparisons between two or more groups. $p < 0.05$ was the cut-off for statistical significance.

5. Conclusions

Given the small sample size, our power to make a definitive conclusion is limited. Nevertheless, some interesting observations still merit attention. When compared with the naturally conceived group, placenta and newborn CBMC from the ICSI group, but not IVF group, showed H3K4me3 alteration. Besides, ICSI-boys present more genes with deH3K4me3 than ICSI-girls. Varying oxygen conditions, Polr2A, and KDM5A impacted H3K4me3 levels. The H3K4me3 alteration, with its potential influence on the development of children, may likely derive from the special manipulation used in the ICSI procedure and/or parental infertility background.

Supplementary Materials: The following are available online at <https://www.mdpi.com/article/10.3390/ijms22168574/s1>, Figure S1: PPI network based on the genes with deH3K4me3 from ICSI-boys. The minimum required interaction score was set as 0.4. PPI, protein-protein interaction; deH3K4me3, differentially enriched tri-methylated-histone-H3-lysine-4; ICSI, intracytoplasmic sperm injection, Figure S2: PPI network based on the genes with deH3K4me3 from ICSI-girls. The minimum required interaction score was set as 0.4, Figure S3: Venn diagrams. (a) Overlapping results of transcription factor analysis for genes with H3K4me3 enrichment in 4-cell, 8-cell, and ICM stages. (b) Overlapping results of literature retrieval and transcription factor analysis for genes H3K4me3 enrichment in 4-cell, 8-cell, and ICM stages. ICM, inner cell mass, Table S1: The list of imprinted genes with entrezID, Table S2: The list of cardiovascular-disease-associated genes with entrezID, Table S3: Clinical characteristics of the study subjects. a Mean \pm Standard Deviation. b ANOVA, analysis of variance. c Fisher’s exact test. BMI = body weight (kg)/body height² (m²). BMI, body mass index. NS, non-significant, Table S4: Genes with deH3K4me3 in IVF and ICSI children. This table showed the comparison results of each gene promoter H3K4me3 read counts between natural conception-boys ($n = 6$) vs. ICSI-boys ($n = 2$), natural conception-boys ($n = 6$) vs. IVF-boys ($n = 4$), natural conception-girls ($n = 6$) vs. ICSI-girls ($n = 4$), and natural conception-girls ($n = 6$) vs. IVF-girls ($n = 4$). The comparison was performed via R package ‘edgeR’. The genes with $|\log FC| > 1$ and $FDR < 0.05$ were selected as “genes with deH3K4me3”, compared with the same-gender natural conception groups. FC, fold change; FDR, false discovery rate; IVF, in vitro fertilization, Table S5: Cardiovascular-disease-associated genes with deH3K4me3 in ICSI children. This table showed the overlapping results of cardiovascular-disease-associated genes and the genes with deH3K4me3 in ICSI children, Table S6: Transcription factor analysis for genes with H3K4me3 enrichment in 4-cell,

8-cell, and ICM stages. Transcription factor analysis was performed via R-package 'RcisTarget'. Motifs with a NES over 3.0 were retained. ICM, inner cell mass; NES, normalized enrichment score; TF, transcription factor; AUC, area under the curve, Table S7: Literature retrieval results for enzymes/proteins that were potentially involved in regulating H3K4me3, Table S8: Transcription factor lists in the Venn diagrams.

Author Contributions: Conceptualization, U.J., V.v.S. and H.Y.; methodology, C.K. and M.R.; formal analysis, H.Y., Z.M. and L.P.; writing—original draft preparation, H.Y.; writing—review and editing, U.J., V.v.S. and S.M.; supervision, U.J. and V.v.S.; project administration, U.J. All authors have read and agreed to the published version of the manuscript.

Funding: This research received no external funding.

Institutional Review Board Statement: The study was conducted according to the guidelines of the Declaration of Helsinki, and approved by the Ethics Committee of Medical Faculty, Ludwig-Maximilians-University Munich (NO.: 337-06, date of approval: 29 December 2006).

Informed Consent Statement: Informed consent was obtained from all subjects involved in the study.

Data Availability Statement: Publicly available datasets were analyzed in this study. These data can be found here: GEO: <https://www.ncbi.nlm.nih.gov/geo/>.

Acknowledgments: The authors would like to thank Thomas Kolben and other clinical staff for placental sample collection. In addition, the authors thank the editors and the anonymous reviewers for constructive comments. Zhi Ma acknowledges the China Scholarship Council (CSC) for supporting his study in Ludwig-Maximilians-University Munich.

Conflicts of Interest: The authors declare no conflict of interest. The funders had no role in the design of the study; in the collection, analyses, or interpretation of data; in the writing of the manuscript, or in the decision to publish the results.

Abbreviations

ARTs	assisted reproductive technologies
BWS	Beckwith-Wiedemann syndrome
SRS	Silver-Russell syndrome
PWS	Prader-Willi syndrome
AS	Angelman syndrome
IVF	in vitro fertilization
ICSI	intracytoplasmic sperm injection
H3K4me3	tri-methylated histone H3 lysine-4
H3K9ac	acetylated histone H3 lysine-9
H3K27ac	acetylated histone H3 lysine-27
CBMC	cord blood mononuclear cell
deH3K4me3	differentially enriched H3K4me3
FC	fold change
FDR	false discovery rate
PPI	protein–protein interaction
SNRPN	<i>Small Nuclear Ribonucleoprotein Polypeptide N</i>
ZFP90	<i>ZFP90 Zinc Finger Protein</i>
DGCR6	<i>DiGeorge Syndrome Critical Region Gene 6</i>
HNF1A	<i>HNF1 Homeobox A</i>
GO	Gene Ontology
Polr2A	RNA polymerase II subunit A
KDM5A	lysine demethylase 5A
TFAP2C	transcription factor AP-2 gamma
KLF15	kruppel like factor 15
SP3	SP3 transcription factor
RARA	retinoic acid receptor alpha
IHC	immunohistochemistry
IRS	immune-reactive score

ICC	Immunocytochemistry
HIF 1 α	hypoxia inducible factor 1 α
ICM	inner cell mass
Pygo2	pygopus 2
PCGF6	polycomb group ring finger 6
IL-13	interleukin-13
Pol II	RNA polymerase II
H ₂ O ₂	hydrogen peroxide
KDM	lysine demethylase
KDM5B	lysine demethylase 5B
co-IP	co-immunoprecipitation
GEO	Gene Expression Omnibus
TSS	transcription start site
IGV	Integrative Genomic Viewer
TF	transcription factor
NES	normalized enrichment score
RIPA	radioimmunoprecipitation assay buffer
SD	standard deviation
ANOVA	one-way analysis of variance

References

- Gosden, R.; Trasler, J.; Lucifero, D.; Faddy, M. Rare congenital disorders, imprinted genes, and assisted reproductive technology. *Lancet* **2003**, *361*, 1975–1977. [[CrossRef](#)]
- Liu, Y.; Gu, Y.; Su, M.; Liu, H.; Zhang, S.; Zhang, Y. An analysis about heterogeneity among cancers based on the DNA methylation patterns. *BMC Cancer* **2019**, *19*, 1–15. [[CrossRef](#)]
- Rexhaj, E.; Paoloni-Giacobino, A.; Rimoldi, S.F.; Fuster, D.G.; Andereg, M.; Somm, E.; Bouillet, E.; Allemann, Y.; Sartori, C.; Scherrer, U. Mice generated by in vitro fertilization exhibit vascular dysfunction and shortened life span. *J. Clin. Investig.* **2013**, *123*, 5052–5060. [[CrossRef](#)] [[PubMed](#)]
- Rexhaj, E.; Bloch, J.; Jayet, P.Y.; Rimoldi, S.F.; Dessen, P.; Mathieu, C.; Tolsa, J.F.; Nicod, P.; Scherrer, U.; Sartori, C. Fetal programming of pulmonary vascular dysfunction in mice: Role of epigenetic mechanisms. *Am. J. Physiol. Heart Circ. Physiol.* **2011**, *301*, H247–H252. [[CrossRef](#)] [[PubMed](#)]
- Market-Velker, B.A.; Fernandes, A.D.; Mann, M.R.W. Side-by-side comparison of five commercial media systems in a mouse model: Suboptimal in vitro culture interferes with imprint maintenance. *Biol. Reprod.* **2010**, *83*, 938–950. [[CrossRef](#)] [[PubMed](#)]
- Uk, A.; Collardeau-Frachon, S.; Scanvion, Q.; Michon, L.; Amar, E. Assisted Reproductive Technologies and imprinting disorders: Results of a study from a French congenital malformations registry. *Eur. J. Med. Genet.* **2018**, *61*, 518–523. [[CrossRef](#)] [[PubMed](#)]
- Lazaraviciute, G.; Kauser, M.; Bhattacharya, S.; Haggarty, P.; Bhattacharya, S. A systematic review and meta-analysis of DNA methylation levels and imprinting disorders in children conceived by IVF/ICSI compared with children conceived spontaneously. *Hum. Reprod. Update* **2014**, *20*, 840–852. [[CrossRef](#)]
- Ghosh, J.; Coutifaris, C.; Sapienza, C.; Mainigi, M. Global DNA methylation levels are altered by modifiable clinical manipulations in assisted reproductive technologies. *Clin. Epigenetics* **2017**, *9*, 1–10. [[CrossRef](#)]
- Kobayashi, H.; Hiura, H.; John, R.M.; Sato, A.; Otsu, E.; Kobayashi, N.; Suzuki, R.; Suzuki, F.; Hayashi, C.; Utsunomiya, T.; et al. DNA methylation errors at imprinted loci after assisted conception originate in the parental sperm. *Eur. J. Hum. Genet.* **2009**, *17*, 1582–1591. [[CrossRef](#)]
- Fernández-Gonzalez, R.; Ramirez, M.A.; Bilbao, A.; De Fonseca, F.R.; Gutiérrez-Adán, A. Suboptimal in vitro culture conditions: An epigenetic origin of long-term health effects. *Mol. Reprod. Dev.* **2007**, *74*, 1149–1156. [[CrossRef](#)]
- De waal, E.; Yamazaki, Y.; Ingale, P.; Bartolomei, M.S.; Yanagimachi, R.; McCarrey, J.R. Gonadotropin stimulation contributes to an increased incidence of epimutations in ICSI-derived mice. *Hum. Mol. Genet.* **2012**, *21*, 4460–4472. [[CrossRef](#)] [[PubMed](#)]
- Turner, B.M. Epigenetic responses to environmental change and their evolutionary implications. *Philos. Trans. R. Soc. B Biol. Sci.* **2009**, *364*, 3403–3418. [[CrossRef](#)] [[PubMed](#)]
- Eastman, A.J.; Xu, J.; Bermik, J.; Potchen, N.; den Dekker, A.; Neal, L.M.; Zhao, G.; Malachowski, A.; Schaller, M.; Kunkel, S.; et al. Epigenetic stabilization of DC and DC precursor classical activation by TNF α contributes to protective T cell polarization. *Sci. Adv.* **2019**, *5*, eaaw9051. [[CrossRef](#)] [[PubMed](#)]
- Zhang, Q.; Bai, B.; Mei, X.; Wan, C.; Cao, H.; Li, D.; Wang, S.; Zhang, M.; Wang, Z.; Wu, J.; et al. Elevated H3K79 homocysteinylation causes abnormal gene expression during neural development and subsequent neural tube defects. *Nat. Commun.* **2018**, *9*, 1–16. [[CrossRef](#)] [[PubMed](#)]
- Huang, X.; Gao, X.; Li, W.; Jiang, S.; Li, R.; Hong, H.; Zhao, C.; Zhou, P.; Chen, H.; Bo, X.; et al. Stable H3K4me3 is associated with transcription initiation during early embryo development. *Bioinformatics* **2019**, *35*, 3931–3936. [[CrossRef](#)]
- Liu, M.; Chen, B.; Pei, L.; Zhang, Q.; Zou, Y.; Xiao, H.; Zhou, J.; Chen, L.; Wang, H. Decreased H3K9ac level of StAR mediated testicular dysplasia induced by prenatal dexamethasone exposure in male offspring rats. *Toxicology* **2018**, *408*, 1–10. [[CrossRef](#)]

17. Xiao, H.; Wen, Y.; Pan, Z.; Shangguan, Y.; Qin, J.; Tan, Y.; Jiang, H.; Li, B.; Zhang, Q.; Chen, L.; et al. Increased H3K27ac level of ACE mediates the intergenerational effect of low peak bone mass induced by prenatal dexamethasone exposure in male offspring rats. *Cell Death Dis.* **2018**, *9*, 1–14. [[CrossRef](#)]
18. Creighton, M.P.; Cheng, A.W.; Welstead, G.G.; Kooistra, T.; Carey, B.W.; Steine, E.J.; Hanna, J.; Lodato, M.A.; Frampton, G.M.; Sharp, P.A.; et al. Histone H3K27ac separates active from poised enhancers and predicts developmental state. *Proc. Natl. Acad. Sci. USA* **2010**, *107*, 21931–21936. [[CrossRef](#)]
19. Okae, H.; Toh, H.; Sato, T.; Hiura, H.; Takahashi, S.; Shirane, K.; Kabayama, Y.; Suyama, M.; Sasaki, H.; Arima, T. Derivation of Human Trophoblast Stem Cells. *Cell Stem Cell* **2018**, *22*, 50–63.e6. [[CrossRef](#)]
20. Gaspar, R.C.; Arnold, D.R.; Corrêa, C.A.P.; da Rocha, C.V.; Pentead, J.C.T.; del Collado, M.; Vantini, R.; Garcia, J.M.; Lopes, F.L. Oxygen tension affects histone remodeling of invitro-produced embryos in a bovine model. *Theriogenology* **2015**, *83*, 1408–1415. [[CrossRef](#)]
21. Belli, M.; Antonouli, S.; Palmerini, M.G.; Bianchi, S.; Bernardi, S.; Khalili, M.A.; Donfrancesco, O.; Nottola, S.A.; Macchiarelli, G. The effect of low and ultra-low oxygen tensions on mammalian embryo culture and development in experimental and clinical IVF. *Syst. Biol. Reprod. Med.* **2020**, *66*, 229–235. [[CrossRef](#)]
22. Bontekoe, S.; Mantikou, E.; van Wely, M.; Seshadri, S.; Repping, S.; Mastenbroek, S. Low oxygen concentrations for embryo culture in assisted reproductive technologies. *Cochrane Database Syst. Rev.* **2012**, *7*, CD008950. [[CrossRef](#)] [[PubMed](#)]
23. Guameri, C.; Restelli, L.; Mangiarini, A.; Ferrari, S.; Somigliana, E.; Paffoni, A. Can we use incubators with atmospheric oxygen tension in the first phase of in vitro fertilization? A retrospective analysis. *J. Assist. Reprod. Genet.* **2015**, *32*, 77–82. [[CrossRef](#)] [[PubMed](#)]
24. Chen, W.; Peng, Y.; Ma, X.; Kong, S.; Tan, S.; Wei, Y.; Zhao, Y.; Zhang, W.; Wang, Y.; Yan, L.; et al. Integrated multi-omics reveal epigenomic disturbance of assisted reproductive technologies in human offspring. *EBioMedicine* **2020**, *61*, 103076. [[CrossRef](#)] [[PubMed](#)]
25. Elliott, G.; Hong, C.; Xing, X.; Zhou, X.; Li, D.; Coarfa, C.; Bell, R.J.A.; Maire, C.L.; Ligon, K.L.; Sigaroudinia, M.; et al. Intermediate DNA methylation is a conserved signature of genome regulation. *Nat. Commun.* **2015**, *6*, 7363. [[CrossRef](#)]
26. Kim, T.H.; Barrera, L.O.; Zheng, M.; Qu, C.; Singer, M.A.; Richmond, T.A.; Wu, Y.; Green, R.D.; Ren, B. A high-resolution map of active promoters in the human genome. *Nature* **2005**, *436*, 876–880. [[CrossRef](#)] [[PubMed](#)]
27. Niu, Y.; Desmarais, T.L.; Tong, Z.; Yao, Y.; Costa, M. Oxidative stress alters global histone modification and DNA methylation. *Free Radic. Biol. Med.* **2015**, *82*, 22–28. [[CrossRef](#)]
28. Guo, X.Y.; Liu, X.M.; Jin, L.; Wang, T.T.; Ullah, K.; Sheng, J.Z.; Huang, H.F. Cardiovascular and metabolic profiles of offspring conceived by assisted reproductive technologies: A systematic review and meta-analysis. *Fertil. Steril.* **2017**, *107*, 622–631.e5. [[CrossRef](#)]
29. Graf, A.E.; Lallier, S.W.; Waidyaratne, G.; Thompson, M.D.; Tipple, T.E.; Hester, M.E.; Trask, A.J.; Rogers, L.K. Maternal high fat diet exposure is associated with increased hepcidin levels, decreased myelination, and neurobehavioral changes in male offspring. *Brain. Behav. Immun.* **2016**, *58*, 369–378. [[CrossRef](#)]
30. Choux, C.; Petazzi, P.; Sanchez-Delgado, M.; Hernandez Mora, J.R.; Monteagudo, A.; Sagot, P.; Monk, D.; Fauque, P. The hypomethylation of imprinted genes in IVF/ICSI placenta samples is associated with concomitant changes in histone modifications. *Epigenetics* **2020**, *15*, 1386–1395. [[CrossRef](#)]
31. Rivera, R.M.; Stein, P.; Weaver, J.R.; Mager, J.; Schultz, R.M.; Bartolomei, M.S. Manipulations of mouse embryos prior to implantation result in aberrant expression of imprinted genes on day 9.5 of development. *Hum. Mol. Genet.* **2008**, *17*, 1–14. [[CrossRef](#)]
32. White, H.E.; Hall, V.J.; Cross, N.C.P. Methylation-sensitive high-resolution melting-curve analysis of the *SNRPN* gene as a diagnostic screen for Prader-Willi and Angelman syndromes. *Clin. Chem.* **2007**, *53*, 1960–1962. [[CrossRef](#)] [[PubMed](#)]
33. Batie, M.; Frost, J.; Frost, M.; Wilson, J.W.; Schofield, P.; Rocha, S. Hypoxia induces rapid changes to histone methylation and reprograms chromatin. *Science* **2019**, *363*, 1222–1226. [[CrossRef](#)]
34. Lee, S.; Lee, J.; Chae, S.; Moon, Y.; Lee, H.Y.; Park, B.; Yang, E.G.; Hwang, D.; Park, H. Multi-dimensional histone methylations for coordinated regulation of gene expression under hypoxia. *Nucleic Acids Res.* **2017**, *45*, 11643–11657. [[CrossRef](#)]
35. Zhou, X.; Sun, H.; Chen, H.; Zavadil, J.; Kluz, T.; Arita, A.; Costa, M. Hypoxia induces trimethylated H3 lysine 4 by inhibition of JARID1A demethylase. *Cancer Res.* **2010**, *70*, 4214–4221. [[CrossRef](#)]
36. Yang, H.; Kuhn, C.; Kolben, T.; Ma, Z.; Lin, P.; Mahner, S.; Jeschke, U.; von Schönfeldt, V. Early life oxidative stress and long-lasting cardiovascular effects on offspring conceived by assisted reproductive technologies: A review. *Int. J. Mol. Sci.* **2020**, *21*, 5175. [[CrossRef](#)] [[PubMed](#)]
37. Agarwal, A.; Said, T.M.; Bedaiwy, M.A.; Banerjee, J.; Alvarez, J.G. Oxidative stress in an assisted reproductive techniques setting. *Fertil. Steril.* **2006**, *86*, 503–512. [[CrossRef](#)]
38. Sazontova, T.G.; Bolotova, A.V.; Bedareva, I.V.; Kostina, N.V.; Arkhipenko, Y.V. Adaptation to intermittent hypoxia/hyperoxia enhances efficiency of exercise training. In *Intermittent Hypoxia and Human Diseases*; Springer: London, UK, 2014; pp. 191–205, ISBN 9781447129066.
39. Jagannathan, L.; Cuddapah, S.; Costa, M. Oxidative Stress under Ambient and Physiological Oxygen Tension in Tissue Culture. *Curr. Pharmacol. Rep.* **2016**, *2*, 64–72. [[CrossRef](#)] [[PubMed](#)]

40. Parker, L.; Shaw, C.S.; Banting, L.; Levinger, I.; Hill, K.M.; McAinch, A.J.; Stepto, N.K. Acute low-volume high-intensity interval exercise and continuous moderate-intensity exercise elicit a similar improvement in 24-h glycemic control in overweight and obese adults. *Front. Physiol.* **2017**, *7*, 661. [[CrossRef](#)] [[PubMed](#)]
41. Bazopoulou, D.; Knoefler, D.; Zheng, Y.; Ulrich, K.; Oleson, B.J.; Xie, L.; Kim, M.; Kaufmann, A.; Lee, Y.T.; Dou, Y.; et al. Developmental ROS individualizes organismal stress resistance and lifespan. *Nature* **2019**, *576*, 301–305. [[CrossRef](#)] [[PubMed](#)]
42. Araki, Y.; Aizaki, Y.; Sato, K.; Oda, H.; Kurokawa, R.; Mimura, T. Altered gene expression profiles of histone lysine methyltransferases and demethylases in rheumatoid arthritis synovial fibroblasts. *Clin. Exp. Rheumatol.* **2018**, *36*, 314–316.
43. Zhou, C.; Zhang, Y.; Dai, J.; Zhou, M.; Liu, M.; Wang, Y.; Chen, X.Z.; Tang, J. Pygo2 functions as a prognostic factor for glioma due to its up-regulation of H3K4me3 and promotion of MLL1/MLL2 complex recruitment. *Sci. Rep.* **2016**, *6*, 22066. [[CrossRef](#)] [[PubMed](#)]
44. Boukhalel, G.M.; Cordeiro, B.; Deblois, G.; Dimitrov, V.; Bailey, S.D.; Holowka, T.; Domi, A.; Guak, H.; Chiu, H.H.C.; Everts, B.; et al. The Transcriptional Repressor Polycomb Group Factor 6, PCGF6, Negatively Regulates Dendritic Cell Activation and Promotes Quiescence. *Cell Rep.* **2016**, *16*, 1829–1837. [[CrossRef](#)]
45. Yu, L.; Li, N.; Zhang, J.; Jiang, Y. IL-13 regulates human nasal epithelial cell differentiation via H3K4me3 modification. *J. Inflamm. Res.* **2017**, *10*, 181–188. [[CrossRef](#)] [[PubMed](#)]
46. Mikhaylova, O.; Ignacak, M.L.; Barankiewicz, T.J.; Harbaugh, S.V.; Yi, Y.; Maxwell, P.H.; Schneider, M.; Van Geyte, K.; Carmeliet, P.; Revelo, M.P.; et al. The von Hippel-Lindau Tumor Suppressor Protein and Egl-9-Type Proline Hydroxylases Regulate the Large Subunit of RNA Polymerase II in Response to Oxidative Stress. *Mol. Cell. Biol.* **2008**, *28*, 2701–2717. [[CrossRef](#)]
47. Li, X.; Wang, T.; Yin, S.; Zhang, G.; Cao, Q.; Wen, X.; Zhang, H.; Wang, D.; Zhu, W. The improved energy metabolism and blood oxygen-carrying capacity for pufferfish, *Takifugu fasciatus*, against acute hypoxia under the regulation of oxygen sensors. *Fish Physiol. Biochem.* **2019**, *45*, 323–340. [[CrossRef](#)]
48. Ignacak, M.L.; Harbaugh, S.V.; Dayyat, E.; Row, B.W.; Gozal, D.; Czyzyk-Krzeska, M.F. Intermittent hypoxia regulates RNA polymerase II in hippocampus and prefrontal cortex. *Neuroscience* **2009**, *158*, 1436–1445. [[CrossRef](#)] [[PubMed](#)]
49. Tufegdžić Vidaković, A.; Mitter, R.; Kelly, G.P.; Neumann, M.; Harreman, M.; Rodríguez-Martínez, M.; Herlihy, A.; Weems, J.C.; Boeing, S.; Encheva, V.; et al. Regulation of the RNAPII Pool Is Integral to the DNA Damage Response. *Cell* **2020**, *180*, 1245–1261.e21. [[CrossRef](#)]
50. Zhao, L.; Wang, S.; Cao, Z.; Ouyang, W.; Zhang, Q.; Xie, L.; Zheng, R.; Guo, M.; Ma, M.; Hu, Z.; et al. Chromatin loops associated with active genes and heterochromatin shape rice genome architecture for transcriptional regulation. *Nat. Commun.* **2019**, *10*, 3640. [[CrossRef](#)]
51. Rea, S.; Eisenhaber, F.; O'Carroll, D.; Strahl, B.D.; Sun, Z.W.; Schmid, M.; Opravil, S.; Mechtler, K.; Ponting, C.P.; Allis, C.D.; et al. Regulation of chromatin structure by site-specific histone H3 methyltransferases. *Nature* **2000**, *406*, 593–599. [[CrossRef](#)]
52. Gallipoli, P.; Huntly, B.J.P. Histone modifiers are oxygen sensors. *Science* **2019**, *363*, 1148–1149. [[CrossRef](#)] [[PubMed](#)]
53. Xia, O.; Lemieux, M.E.; Li, W.; Carroll, J.S.; Brown, M.; Shirley Liu, X.; Kung, A.L. Integrative analysis of HIF binding and transactivation reveals its role in maintaining histone methylation homeostasis. *Proc. Natl. Acad. Sci. USA* **2009**, *106*, 4260–4265. [[CrossRef](#)]
54. Dahl, J.A.; Jung, I.; Aanes, H.; Greggains, G.D.; Manaf, A.; Lerdrup, M.; Li, G.; Kuan, S.; Li, B.; Lee, A.Y.; et al. Broad histone H3K4me3 domains in mouse oocytes modulate maternal-to-zygotic transition. *Nature* **2016**, *537*, 548–552. [[CrossRef](#)]
55. Penterling, C.; Drexler, G.A.; Böhländ, C.; Stamp, R.; Wilke, C.; Braselmann, H.; Caldwell, R.B.; Reindl, J.; Girst, S.; Greubel, C.; et al. Depletion of histone demethylase *jarid1a* resulting in histone hyperacetylation and radiation sensitivity does not affect DNA double-strand break repair. *PLoS ONE* **2016**, *11*, e0156599. [[CrossRef](#)] [[PubMed](#)]
56. Huang, J.; Zhang, H.; Wang, X.; Dobbs, K.B.; Yao, J.; Qin, G.; Whitworth, K.; Walters, E.M.; Prather, R.S.; Zhao, J. Impairment of preimplantation porcine embryo development by histone demethylase KDM5B knockdown through disturbance of bivalent H3K4me3-H3K27me3 modifications. *Biol. Reprod.* **2015**, *92*, 72. [[CrossRef](#)]
57. Remmele, W.; Stegner, H.E. Recommendation for uniform definition of an immunoreactive score (IRS) for immunohistochemical estrogen receptor detection (ER-ICA) in breast cancer tissue. *Pathologie* **1987**, *8*, 138–140. [[PubMed](#)]
58. Petry, C.J.; Marcos, N.S.; Pimentel, G.; Hayes, M.G.; Nodzinski, M.; Scholtens, D.M.; Hughes, I.A.; Acerini, C.L.; Ong, K.K.; Lowe, W.L.; et al. Associations between Fetal Imprinted Genes and Maternal Blood Pressure in Pregnancy. *Hypertension* **2016**, *68*, 1459–1466. [[CrossRef](#)]
59. Moore, G.E.; Ishida, M.; Demetriou, C.; Al-Olabi, L.; Leon, L.J.; Thomas, A.C.; Abu-Amro, S.; Frost, J.M.; Stafford, J.L.; Chaoqun, Y.; et al. The role and interaction of imprinted genes in human fetal growth. *Philos. Trans. R. Soc. B Biol. Sci.* **2015**, *370*, 20140074. [[CrossRef](#)]
60. Vidal, A.C.; Murphy, S.K.; Murtha, A.P.; Schildkraut, J.M.; Soubry, A.; Huang, Z.; Neelon, S.E.B.; Fuemmeler, B.; Iversen, E.; Wang, F.; et al. Associations between antibiotic exposure during pregnancy, birth weight and aberrant methylation at imprinted genes among offspring. *Inf. J. Obs.* **2013**, *37*, 907–913. [[CrossRef](#)]

Huixia Yang, Zhi Ma, Lin Peng, Christina Kuhn, Martina Rahmeh, Sven Mahner, Udo Jeschke, Viktoria von Schönfeldt. Comparison of Histone H3K4me3 between IVF and ICSI Technologies and between Boy and Girl Offspring. *Int J Mol Sci.* 2021 Aug 9;22(16):8574. doi: 10.3390/ijms22168574.

6. Paper II



biomedicines



Article

FAM111A Is a Novel Molecular Marker for Oocyte Aging

Huixia Yang ¹, Thomas Kolben ¹, Mirjana Kessler ¹, Sarah Meister ¹, Corinna Paul ¹, Julia van Dorp ¹, Sibel Eren ¹, Christina Kuhn ^{1,2}, Martina Rahmeh ¹, Cornelia Herbst ¹, Sabine Gabriele Fink ¹, Gabriele Weimer ¹, Sven Mahner ¹, Udo Jeschke ^{1,2,*} and Viktoria von Schönfeldt ¹

¹ Department of Obstetrics and Gynecology, University Hospital, Ludwig-Maximilians-University, 81377 Munich, Germany; huixia.yang@med.uni-muenchen.de (H.Y.); thomas.kolben@med.uni-muenchen.de (T.K.); mirjana.kessler@med.uni-muenchen.de (M.K.); sarah.meister@med.uni-muenchen.de (S.M.); corinna.paul@med.uni-muenchen.de (C.P.); julia.van.dorp@hotmail.de (J.v.D.); sibel.eren@med.uni-muenchen.de (S.E.); christina.kuhn@uk-augsburg.de (C.K.); martina.rahmeh@med.uni-muenchen.de (M.R.); cornelia.herbst@med.uni-muenchen.de (C.H.); s.fink@med.uni-muenchen.de (S.G.F.); gabriele.weimer@med.uni-muenchen.de (G.W.); sven.mahner@med.uni-muenchen.de (S.M.); viktoriaschoenfeldt@med.uni-muenchen.de (V.v.S.)

² Department of Obstetrics and Gynecology, University Hospital Augsburg, 86156 Augsburg, Germany

* Correspondence: udo.jeschke@med.uni-muenchen.de; Tel.: +49-821-400-165505



Citation: Yang, H.; Kolben, T.; Kessler, M.; Meister, S.; Paul, C.; van Dorp, J.; Eren, S.; Kuhn, C.; Rahmeh, M.; Herbst, C.; et al. *FAM111A* Is a Novel Molecular Marker for Oocyte Aging. *Biomedicines* **2022**, *10*, 257. <https://doi.org/10.3390/biomedicines10020257>

Academic Editor: Makoto C. Nagano

Received: 18 November 2021

Accepted: 17 January 2022

Published: 25 January 2022

Publisher's Note: MDPI stays neutral with regard to jurisdictional claims in published maps and institutional affiliations.



Copyright: © 2022 by the authors. Licensee MDPI, Basel, Switzerland. This article is an open access article distributed under the terms and conditions of the Creative Commons Attribution (CC BY) license (<https://creativecommons.org/licenses/by/4.0/>).

Abstract: Aging is the main cause of decline in oocyte quality, which can further trigger the failure of assisted reproductive technology (ART). Exploring age-related genes in oocytes is an important way to investigate the molecular mechanisms involved in oocyte aging. To provide novel insight into this field, we performed a pooled analysis of publicly available datasets, using the overlapping results of two statistical methods on two Gene Expression Omnibus (GEO) datasets. The methods utilized in the current study mainly include Spearman rank correlation, the Wilcoxon signed-rank test, *t*-tests, Venn diagrams, Gene Ontology (GO), Protein–Protein Interaction (PPI), Gene Set Enrichment Analysis (GSEA), Gene Set Variation Analysis (GSVA), and receiver operating characteristic (ROC) curve analysis. We identified hundreds of age-related genes across different gene expression datasets of in vitro maturation-metaphase II (IVM-MII) oocytes. Age-related genes in IVM-MII oocytes were involved in the biological processes of cellular metabolism, DNA replication, and histone modifications. Among these age-related genes, *FAM111A* expression presented a robust correlation with age, seen in the results of different statistical methods and different datasets. *FAM111A* is associated with the processes of chromosome segregation and cell cycle regulation. Thus, this enzyme is potentially an interesting novel marker for the aging of oocytes, and warrants further mechanistic study.

Keywords: oocyte aging; cellular metabolism; DNA replication; histone modifications; cell cycle; WNT signaling pathway; *FAM111A*

1. Introduction

Female fertility decreases progressively with age. It has been revealed that the fertility of a woman in her mid-30s is only half of the fertility potential of a woman in her mid-20s; and this is reduced to less than 5% for a woman in her 40s [1]. The decrease in fertility is reflected in the lower quantity and quality of oocytes. Age-related decline in oocyte quality is an important non-male cause of assisted reproductive technology (ART) failures, and there is no successful treatment for the age-related decline in oocyte quality [2]. Increased aneuploidy is an important cause of the decline in oocyte quality [3]. In addition, oocyte quality decline has also been associated with nuclear and mitochondrial DNA damage [4,5], meiotic spindle abnormalities, chromosomal misalignment, mitochondrial dysfunction [6], telomere shortening [7], and abnormal structure of the zona pellucida [8,9] and nucleolus [10].

To date, several investigations have explored the influence of maternal age on oocyte gene expression, using microarray and RNA-seq technology. Of these, most have been single-center studies on one or two types of oocytes, with limited sample size. Different analysis methods were used in each study, and the results of these studies remain controversial. Some studies reported that gene expression data for the human germinal vesicle (GV) oocytes [11,12], from women across age groups, remained stable; while others revealed that gene expression among GV oocytes [13], in vivo ovulation-metaphase II (IVO-MII) oocytes [14–17], and in vitro maturation-metaphase II (IVM-MII) oocytes [12,13], were significantly influenced by maternal age. To obtain more generalizable results, multi-center studies with large sample sizes are required.

Given the above research background, in this study, we performed an integrative analysis of the available datasets. The data were derived from two original Gene Expression Omnibus (GEO) datasets, which provide gene expression profiles of oocytes from women of various ages. These two datasets were deposited, respectively, by Reyes et al. [12] and Llonch et al. [13]. In the study of Reyes et al. [12], age was treated as a categorical variable, and differential gene expression analysis between young and old groups was performed using the DESeq2 package. In the study of Llonch et al. [13], age was treated as a continuous variable, and Pearson correlation was applied to investigate the association between gene expression and age. In the current study, age was treated as a categorical variable, and the overlapping results of limma moderated *t*-tests and Spearman correlation were obtained. The primary aim of this study was to explore oocyte age-related genes, which were validated in a second dataset, and to investigate the potential biological functions affected by these age-related genes using functional enrichment analysis. We believe our results provide more reliable insight into understanding the molecular mechanisms underlying the age-related decline in oocyte quality, which may facilitate the development of targeted treatments designed to improve oocyte quality.

2. Materials and Methods

2.1. Data Download and Processing

Gene expression profiles of oocytes (Accession No. GSE95477 [12], GSE158802 [13], and GSE87201 [17]) were obtained from the NCBI GEO (<http://www.ncbi.nlm.nih.gov/geo/>, accessed on 9 August 2021) database. Data processing included quantile normalization and log₂-transformation. All R packages were run in R software (version 4.1.0).

2.2. Age-Related Analysis

Next, as oocyte quality declines with age, we treated age as a categorical variable (using median age to stratify the oocytes), and examined the correlation between age and gene expression by performing Spearman rank correlation, using the R function 'cor.test'. For each detected gene, the Spearman correlation value (*r*) and *p*-value were calculated. Genes with absolute value *r* > 0.3 and *p*-value < 0.05 were considered significantly correlated with age.

Differential gene expression analysis between young and old groups was performed using R package 'limma' (version 3.44.3) [18] and moderated *t*-tests. Genes with absolute fold change (FC) value > 2 and *p*-value < 0.05 were considered significant.

Then, Venn diagrams were generated using 'jvenn' [19] in order to visualize the overlapping results of Spearman rank correlation and *t*-tests, for IVM-MII oocytes from GSE95477 (referred to as Group I in the current study) and GSE158802 (referred to as Group II in the current study).

Based on the overlapping results presented in the Venn diagrams, the overlapping age-related genes in different IVM-MII oocytes were further validated for GV oocytes from GSE158802 (referred to as Group III in the current study) and IVO-MII oocytes from GSE87201 (referred to as Group IV in the current study), using the same methods and parameters as described above.

2.3. Gene Ontology (GO) Functional Enrichment Analysis

To gain an insight into the biological functions of the age-associated genes, Gene Ontology (GO) functional enrichment analysis was performed using package ‘ClusterProfiler’ (version 3.12.0) [20], with the overlapping age-related genes as the input gene list. The R packages ‘ggplot2’ (version 3.3.3) [21] and ‘GOplot’ (version 1.0.2) [22] were used to plot the results. GO categories with p -value < 0.05 were considered as significantly enriched.

2.4. The Capability of Hub Gene *FAM111 Trypsin-like Peptidase A (FAM111A)* for Distinguishing Young and Old Oocytes

The *FAM111 Trypsin-Like Peptidase A (FAM111A)* expression levels between young and old groups were compared using t -tests (for normally distributed expression data) or Wilcoxon signed-rank tests (for non-normally distributed expression data) in R package ‘ggpubr’ (version 0.4.0) [23].

Receiver operating characteristic (ROC) curves and the area under the curve (AUC) were obtained via R package ‘pROC’ (version 1.15.3) [24] and visualized using R package ‘ggplot2’ (version 3.3.3) [21]. The AUC had values generally ranging between 0.5 and 1. Typically, AUC results are categorized as ‘uninformative’ (AUC = 0.5), ‘less accurate’ ($0.5 < \text{AUC} \leq 0.7$), ‘moderately accurate’ ($0.7 < \text{AUC} \leq 0.9$), or ‘very accurate’ ($0.9 < \text{AUC} < 1$) [25].

2.5. Gene Set Enrichment Analysis (GSEA) and Gene Set Variation Analysis (GSVA)

To explore the association between *FAM111A* expression and biological processes/signaling pathways, Gene Set Enrichment Analysis (GSEA) and Gene Set Variation Analysis (GSVA) were carried out, with *FAM111A* as the input gene list. GSEA is a computational method for determining whether a given gene set exerts statistically significant and concordant differences between two cohorts/phenotypes [26]. GSEA analyses of IVM-MII oocytes from Group I (GSE95477) and Group II (GSE158802) were performed using ‘ClusterProfiler’ (version 3.12.0) [20] with default parameters. Terms with p -value < 0.05 were considered statistically significant. GSVA is a non-parametric and unsupervised algorithm that transforms genes in a sample matrix into pre-defined gene sets, without the need for knowing in advance the experiment design [27]. GSVA analyses of IVM-MII oocytes from Group II (GSE158802) were individually implemented via the R package ‘GSVA’ (version 1.30.0) [27] with default parameters. Terms with p -value < 0.05 and absolute value $r > 0.3$ were considered significant. All GO and KEGG related gene sets were obtained from the Molecular Signature Database (MsigDB, <http://software.broadinstitute.org/gsea/msigdb/>, accessed on 28 August 2021).

2.6. Protein–Protein Interaction (PPI) Network Based on *FAM111A*

Protein–Protein Interaction (PPI) networks were constructed for *FAM111A* and its interacting proteins using the GeneMANIA database [28]. GeneMANIA is a user-friendly and regularly updated web interface for predicting gene function, analyzing gene lists, and extending the given gene list with genes of similar function using available proteomics and genomics data [29]. It has been widely applied in the study of PPI relationships. The PPI networks were constructed in terms of co-expression, physical interaction, co-localization, genetic interaction, common pathways, shared protein domains, etc.

2.7. Correlation Analysis of *FAM111A* and Its Interacting Proteins

To explore the potential association between *FAM111A* and its interacting proteins, gene expression profiles of *FAM111A* and its interacting proteins were extracted from oocytes from Group I and Group II. R package ‘SVA’ (version 3.32.1) [30] was used to remove batch effects. The gene–gene correlation matrix between *FAM111A* and its interacting partners was generated using R package ‘corrplot’ (version 0.84) [31] with Spearman correlations. Genes with absolute value $r > 0.3$ and p -value < 0.05 were considered significantly correlated.

3. Results

A summary of the gene expression profiles included in the current analysis is shown in Figure 1A, and Figure 1B presents an overview of the analysis procedures of the study. Based on the median age of each group, the oocytes were stratified into young and old oocytes. The rationale for using the median age to stratify young and old oocytes is the same as that for female fertility, with a downward trend continuing with age. The major objective of our study is to explore the differences presented by oocytes that are already visible at the molecular level.

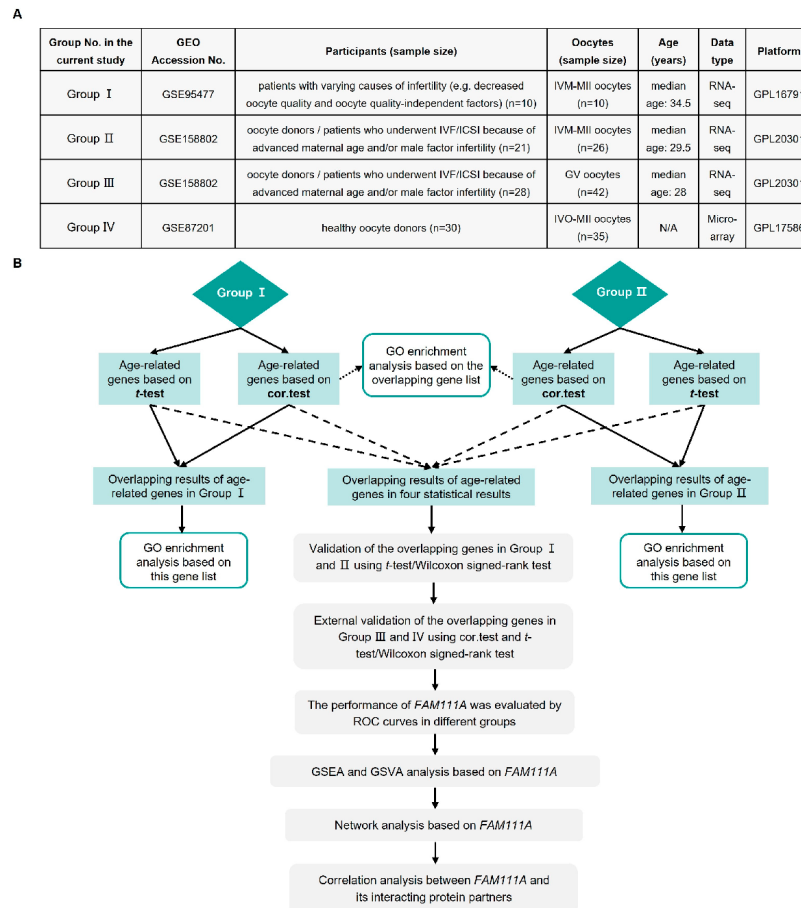


Figure 1. Summary of the present study. (A) Groups included in the analysis of this study. (B) Flowchart of this study. GEO, Gene Expression Omnibus; IVF/ICSI, in vitro fertilization/intracytoplasmic sperm injection; IVM-MII, in vitro maturation-metaphase II; GV, germinal vesicle; IVO-MII, in vivo ovulation-metaphase II; N/A, not available; cor.test, Spearman rank correlation; GO, Gene Ontology; ROC, receiver operating characteristic; GSEA, Gene Set Enrichment Analysis; GSVA, Gene Set Variation Analysis; *FAM111A*, *FAM111 Trypsin-Like Peptidase A*.

3.1. Impact of Age on the Gene Expression of Human Oocytes

Based on Spearman correlation, IVM-MII oocytes from Group I (GSE95477) and Group II (GSE158802) presented 1322 and 933 genes, respectively, showing altered expression with age (Supplementary Tables S1 and S2). Based on *t*-tests, IVM-MII oocytes from Group I and Group II presented, respectively, 377 and 480 genes, with different expression levels between young and old oocytes (Supplementary Tables S3 and S4).

We used Venn diagrams (Figure 2) to identify age-related genes with overlapping Spearman correlation and *t*-test results. There were 249 age-related genes with overlapping results in oocytes from Group I (Figure 2B), 397 age-related genes with overlapping results in oocytes from Group II (Figure 2C), and three age-related genes with overlapping results (*FAM111A*, *Isopentenyl-Diphosphate Delta Isomerase 1 (IDI1)*, and *Lymphocyte Antigen 6 Family Member K (LY6K)*) in all the analysis results (Figure 2D,E).

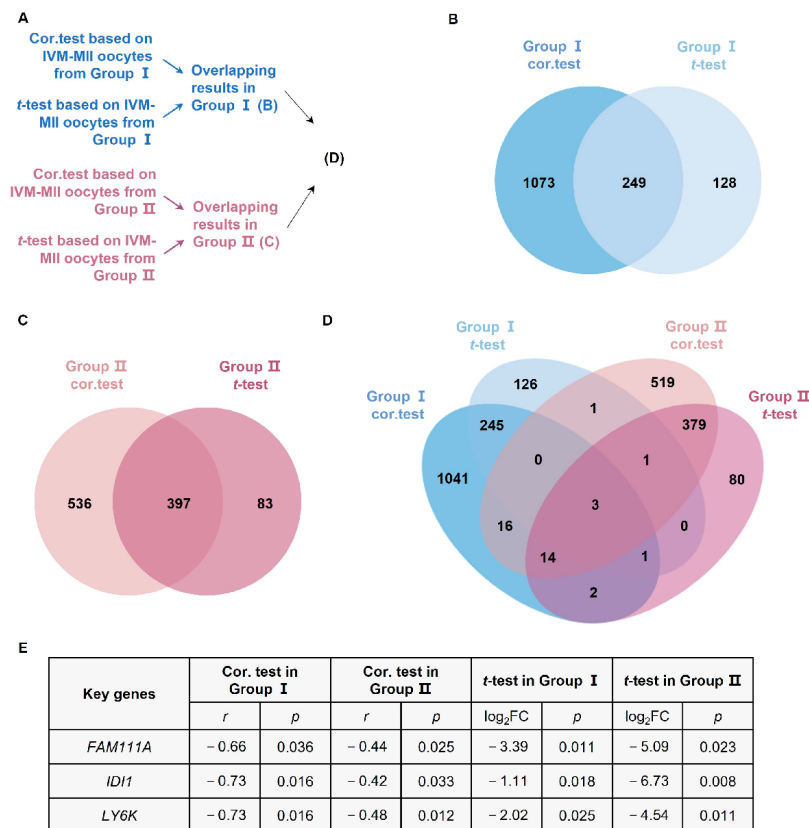


Figure 2. Analysis of age-related genes. (A) Flowchart of the age-related analysis. (B) Overlapping results of cor.test and *t*-test for IVM-MII oocytes from Group I. (C) Overlapping results of cor.test and *t*-test for IVM-MII oocytes from Group II. (D) Overlapping results of age-related genes in Group I and Group II. (E) Based on the cor.test and *t*-test, *FAM111A*, *IDI1*, and *LY6K* are the statistically significant age-related genes in both Group I and Group II. *IDI1*, *Isopentenyl-Diphosphate Delta Isomerase 1*; *LY6K*, *Lymphocyte Antigen 6 Family Member K*. FC, fold change.

To test the validity of our findings (i.e., three overlapping age-related genes), we analyzed GV oocytes from Group III and IVO-MII oocytes from Group IV, and confirmed the correlation of *FAM111A* with age. The correlation coefficients of *FAM111A*, *ID11*, and *LY6K* were, respectively, -0.32 ($p = 0.039$), -0.11 ($p = 0.470$), and 0.08 ($p = 0.602$), in Group III. The correlation coefficients of *FAM111A*, *ID11*, and *LY6K* in Group IV were, respectively, 0.34 ($p = 0.046$), 0.05 ($p = 0.796$), and -0.09 ($p = 0.605$).

3.2. Cellular Metabolism, DNA Replication, and Histone Modifications Are the Biological Processes Enriched by Age-Related Genes in Two Datasets

GO enrichment analysis, based on the age-related genes with overlapping Spearman correlation and *t*-test results, revealed that cellular metabolism, DNA replication, and histone modifications were the biological processes significantly affected by age in both Group I (Figure 3A) and Group II (Figure 3B). GO enrichment analysis, based on the age-related genes with overlapping Spearman correlation results from Group I and Group II, also revealed that biological processes, such as the oxidation of fatty acids/lipids, fatty acid catabolic process, and histone modifications, were significantly influenced by age (Figure 4).

3.3. FAM111A Is the Hub Age-Related Gene in In Vitro Maturation-Metaphase II (IVM-MII) Oocytes and FAM111A Expression Is also Correlated with Age in Germinal Vesicle (GV) and In Vivo Ovulation-Metaphase II (IVO-MII) Oocytes

Based on *t*-test and Wilcoxon signed-rank test results, we found that *FAM111A* expression not only showed significant differences between young and old oocytes from Group I (Figure 5A) and Group II (Figure 5B), but also showed significant differences in GV oocytes from Group III (Figure 5C) and IVO-MII oocytes from Group IV (Figure 5D). Based on the ROC analysis, *FAM111A* showed good discrimination between young and old oocytes (Figure 5E–H).

3.4. Chromosome Segregation and Regulation of Cell Cycle Are the Main Pathways Regulated by FAM111A in IVM-MII Oocytes

Based on the overlapping results of the GSEA analysis of IVM-MII oocytes from Group I (Supplementary Table S5) and Group II (Supplementary Table S6), and GSVA analysis of IVM-MII oocytes from Group II (Supplementary Table S7), meiotic chromosome segregation, the regulation of the cell cycle, the positive regulation of the WNT signaling pathway, actin filament organization, and microtubule-associated complex, were terms significantly regulated by *FAM111A* (Table 1).

3.5. Predicted FAM111A-Associated Protein Includes Zinc Finger Protein 226 (ZNF226), Which Functions in Transcriptional Regulation

We used the GeneMANIA database to analyze the *FAM111A*-associated proteins (Figure 6A). These proteins were predicated based on a highly adaptive algorithm and hundreds of datasets, which were collected from ten publicly available databases, such as GEO, BioGRID, Interologous Interaction Database (I2D), and Pathway Commons [29]. The results reveal that *FAM111A* interacted with Proliferating Cell Nuclear Antigen (PCNA), Mediator Complex Subunit 18 (MED18), Zinc Finger Protein 226 (ZNF226), Nicastrin (NCSTN), and Kringle Containing Transmembrane Protein 2 (KREMEN2), etc. Further, Spearman correlation analysis of the *FAM111A*-associated proteins, based on the gene expression profiles of the oocytes, revealed a borderline correlation between *FAM111A* and *ZNF226* (correlation coefficient $r = 0.32$; $p = 0.054$) (Figure 6B).

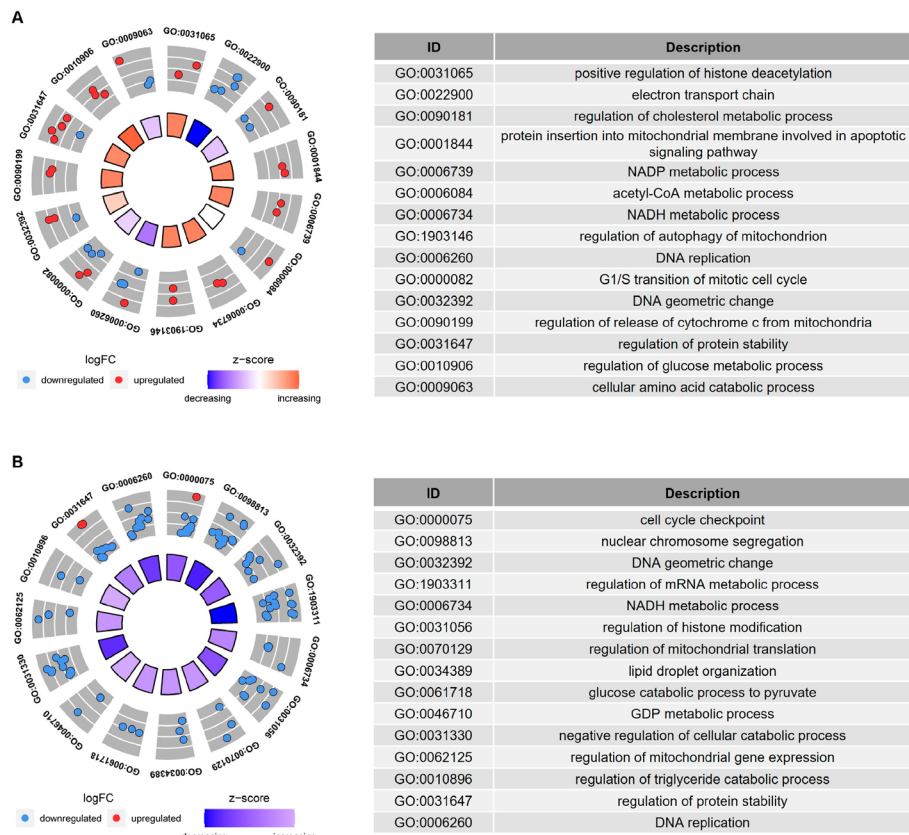


Figure 3. GO enrichment analysis of the age-related genes in IVM-MII oocytes from (A) Group I and (B) Group II. The age-related genes in this analysis were obtained from the overlapping cor.test and *t*-test results. The inner circle in the left figure indicates the Z-score value. The outer ring represents the significantly enriched terms, and the most upregulated and downregulated genes. The blue dot indicates the downregulated gene and the red dot indicates the upregulated gene. The right figure is the description of the enriched GO terms.

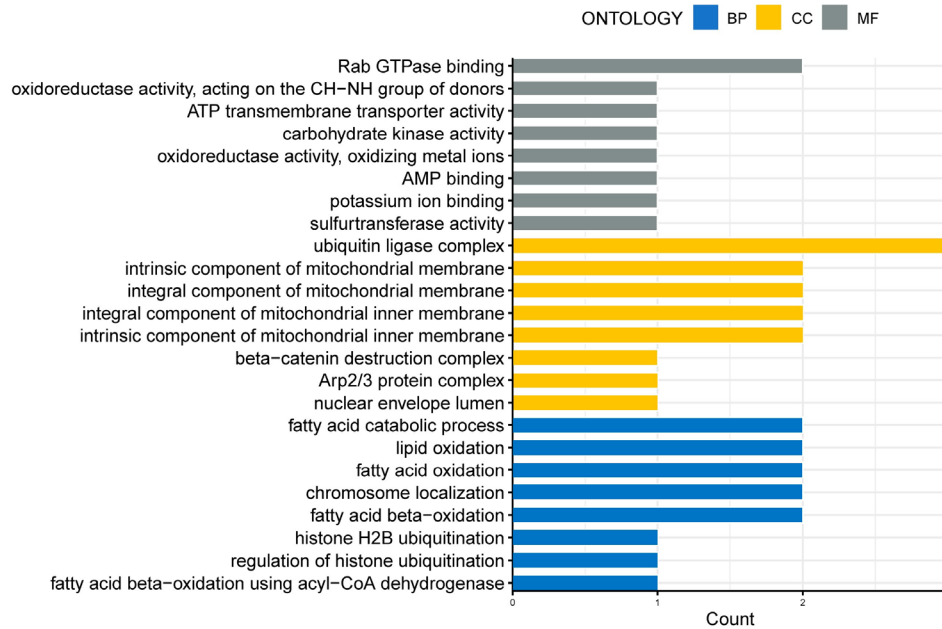


Figure 4. GO enrichment analysis of the overlapping age-related genes in IVM-MII oocytes from Group I and Group II. The age-related genes in this analysis were obtained from the overlapping results of cor.test in Group I and Group II. The x-axis represents the counts of the genes enriched in GO terms. The y-axis represents the significantly enriched terms in BP, CC, and MF. BP, biological process; CC, cellular component; MF, molecular function.

Table 1. The terms overlapping in the results of GSEA and GSVA based on IVM-MII oocytes.

IVM Terms	GSEA of Group I		GSEA of Group II		GSVA of Group II	
	NES	<i>p</i>	NES	<i>p</i>	<i>r</i>	<i>p</i>
GO_MEIOTIC_CHROMOSOME_SEGREGATION	1.65	0.003	1.48	0.004	0.43	0.030
GO_CONDENSED_NUCLEAR_CHROMOSOME_CENTROMERIC_REGION	1.53	0.038	1.71	0.003	0.61	<0.001
GO_CHROMOSOME_LOCALIZATION	1.66	0.004	1.40	0.018	0.44	0.024
GO_REGULATION_OF_CELL_CYCLE_G2_M_PHASE_TRANSITION	1.41	0.010	1.44	<0.001	0.47	0.015
GO_ACTIN_FILAMENT_ORGANIZATION	1.36	0.009	1.36	<0.001	0.51	0.008
GO_POSITIVE_REGULATION_OF_WNT_SIGNALING_PATHWAY	1.39	0.019	1.45	<0.001	0.43	0.028
GO_MICROTUBULE_ASSOCIATED_COMPLEX	1.40	0.019	1.43	0.002	0.53	0.006
GO_PROTEASOME_ACCESSORY_COMPLEX	1.75	0.006	1.52	0.021	0.43	0.027
GO_EXODEOXYRIBONUCLEASE_ACTIVITY	1.71	0.010	1.46	0.038	0.49	0.011

NES > 0, the terms were positively regulated by *FAM111A*; *r* > 0, the terms were positively correlated with *FAM111A*. NES, normalized enrichment score.

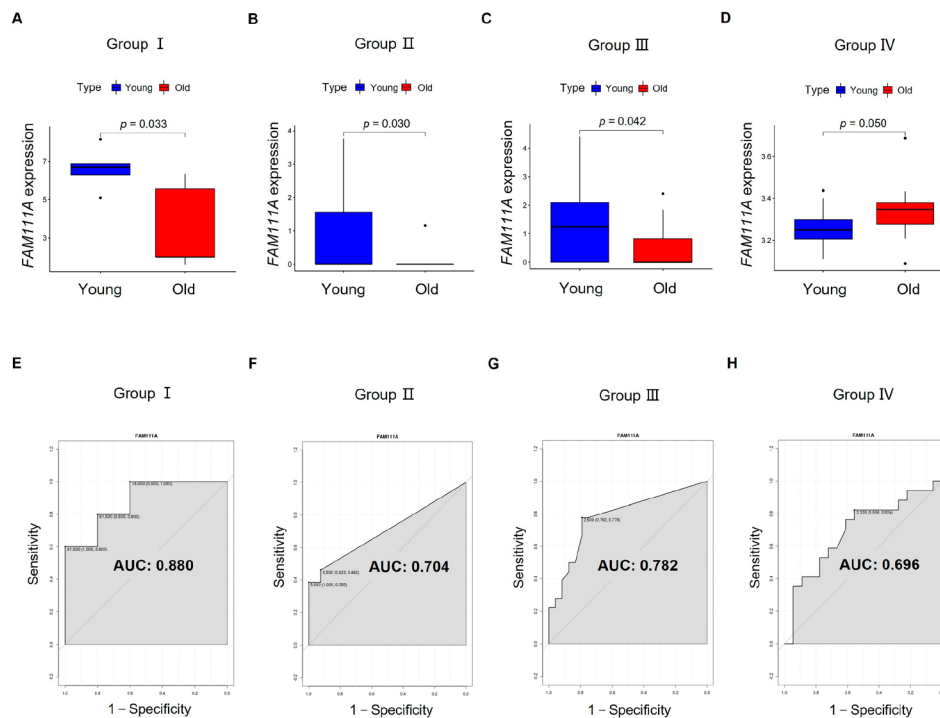


Figure 5. The capability of *FAM111A* for distinguishing young and old oocytes. The expression of *FAM111A* in the oocytes from young and old groups is visualized in (A) Group I and (B) Group II, and further validated in (C) Group III and (D) Group IV. The x-axis represents young and old oocytes. The y-axis represents *FAM111A* expression. *p*-values were calculated using a *t*-test or Wilcoxon signed-rank test. ROC curves are visualized in (E) Group I, (F) Group II, (G) Group III, and (H) Group IV. The x-axis of the ROC graph represents 1—specificity, and the y-axis represents sensitivity. AUC, area under the curve.

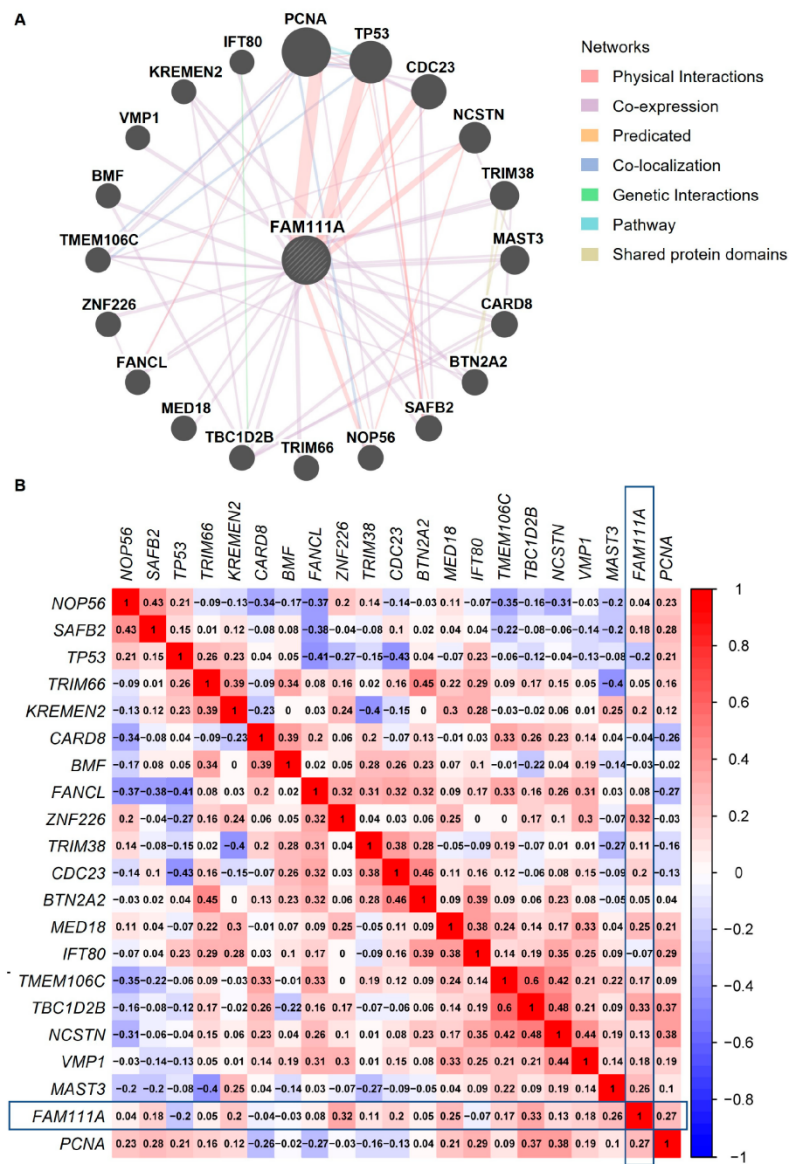


Figure 6. The PPI network and correlation analysis between FAM111A and its interacting protein partners. **(A)** The PPI network of FAM111A and its interacting protein partners. **(B)** Spearman gene-gene correlation matrix between FAM111A and its interacting partners. In the matrix, red and blue represent positive and negative correlations, respectively. The number in each square indicates the Spearman correlation coefficient (*r*-value). PPI, Protein–Protein Interaction.

4. Discussion

In this study, we explored the influence of age on oocytes at the gene expression level. To increase the robustness of our findings, we explored the age-related genes using two statistical methods; moreover, we attempted to identify overlapping results by combining two independent datasets. We found hundreds of genes with significantly altered expression levels between oocytes from young and old age groups; the biological processes influenced by these genes mainly included cellular metabolism, DNA replication, and histone modifications. Among these age-related genes, *FAM111A* expression displayed robust correlations with age in the different statistical methods and different datasets. To our knowledge, this is the first report of a potential gene marker for human oocyte aging. We found that *FAM111A* may be involved in the biological processes associated with chromosome segregation and the regulation of the cell cycle. *FAM111A* protein could potentially interact with regulators of transcription (i.e., ZNF226) and transcription factors (i.e., PCNA).

We identified 249 overlapping age-related genes in oocytes from Group I, and 397 overlapping age-related genes in oocytes from Group II. Based on GO enrichment analysis, we found these two gene lists were both enriched in biological processes associated with cellular metabolism, DNA replication, and histone modifications. The overlapping genes, from Spearman rank correlation, in oocytes from Group I and Group II were also enriched in the terms of the oxidation of fatty acids/lipids, fatty acid catabolic process, and histone modifications. Similarly, Duncan et al. found that age-associated gene signatures in mouse oocytes were involved in the alteration of protein metabolism [10]. Another study, based on liquid and gas chromatography coupled to mass spectrometry, also found that total free fatty acids were decreased in old equine oocytes compared with young oocytes. Furthermore, through the quantification of aerobic and anaerobic metabolism, these researchers found that the metabolic activity of equine oocytes was impaired by maternal aging [32]. Fatty acids are vital substrates for early reproductive events (e.g., oocyte maturation [33,34] and embryo implantation [35]). Upon demand, the metabolism of lipids provides a good source of energy during oocyte maturation. For example, during pig oocyte maturation, fatty acids in lipid droplets (LDs) provide adenosine triphosphate (ATP) via β -oxidation, serving as an energy source for oocytes [36]. The lipid modulators have been investigated to improve the developmental competence of oocytes and embryos in animal models [37]. Modifications to LD morphology and lipid metabolism during the period of oocyte maturation have been revealed to possibly interfere with monospermic fertilization and embryo development in the pig model [38,39]. It has been revealed that the degradation of LDs tends to be via the lipolysis of triacylglycerols to fatty acyl-CoA by lipases at the surface of the LDs, which is often in preparation for mitochondrial metabolism [40].

Corroborating our results, the alteration of histone methylation [41,42] and histone acetylation [43–45] has been reported in old mammalian oocytes. Altered histone modifications usually correlated with changes in chromatin configuration and gene transcription activity [46], which may affect oocyte fertilization and embryo development [44]. For example, decreased histone 4 lysine 20 tri-methylation (H4K20me3) results in chromosomal segregation defects in cell culture [47]. The inhibitor of histone deacetylase during IVM contributes to the reduced developmental potential of bovine oocytes [48]. Notably, epigenetic changes have been regarded as a hallmark of aging, besides telomere shortening [49]. However, studies of age-related epigenetic changes in oocytes are still finite, and, therefore, further studies on this topic are highly awaited.

We identified *FAM111A* as the most robust gene that presented altered gene expression during aging. The overlapping results of GSEA and GSVA analysis based on *FAM111A* revealed that chromosome segregation and regulation of the cell cycle were the main pathways regulated by *FAM111A* in IVM-MII oocytes from both datasets. Other studies on human oocytes [13,50] have come to similar conclusions, that transcripts associated with chromosome segregation and cell cycle regulation are altered during oocyte aging. Fine et al. revealed that *FAM111A* expression is cell-cycle-dependent in cell-cycle-synchronized T98G cells [51]. *FAM111A* is a chymotrypsin-like serine protease, and displays autocleavage

activity in vivo [52]. It has been revealed that *FAM111A* is important for DNA replication [52,53] and plays a role in viral restriction [51,54]. Furthermore, it is hypothesized that *FAM111A* might engage in DNA binding [52], as it localizes to replication forks [55]. Nevertheless, until now, the functions of *FAM111A* remain largely unclarified and require further investigation.

We also found that the WNT signaling pathway was positively regulated by *FAM111A* in IVM-MII oocytes, and that *FAM111A* expression was decreased in aging IVM-MII oocytes. Similarly, a recent study also found that the WNT signaling was downregulated in low-quality rescue IVM (rIVM) oocytes, and revealed that down-regulation of the GATA-1/CREB1/WNT signaling axis might result in the poor maturation performance of rIVM oocytes [56]. This might indicate the existence of a potential link between *FAM111A* expression and WNT signaling, which needs to be further investigated. The WNT signaling pathway is a highly conserved pathway. It plays a major role in cell and tissue maintenance, polarity, and differentiation [57], as well as in maintaining female germ cell survival [58]; furthermore, it is frequently dysregulated in human cancers [59]. The canonical WNT pathway is initiated by WNT proteins [60], which have been revealed as being responsible for regulating the cell cycle and deciding cell fate [61].

Furthermore, based on our PPI network results, we found that *FAM111A* protein may have interactions with ZNF226 and PCNA. The Spearman correlation analysis based on the gene expression profiles from Group I and Group II also revealed a borderline positive correlation between *FAM111A* expression and ZNF226 expression. PCNA is a transcription factor that promotes DNA polymerase delta binding to DNA [62], and plays an essential role in DNA replication, DNA repair [63], and cell cycle regulation [62]. It has also been reported that ZNF226 plays a vital role in transcriptional regulation [64]. Our finding reveals a potential link between transcriptional regulation and oocyte aging.

Though the same statistical methods were used in different datasets, there was still variation in age-related genes between the different datasets, with relatively few overlapping results. This could be due to differences in sequencing methods and coverage of the sequencing platforms, as well as differing age ranges and sources of the study participants. In addition, for the in vitro maturation of oocytes, no unified IVM protocols are established across different in vitro fertilization (IVF) centers [65]. However, differences in methods of follicular priming, time of oocyte retrieval, choices of IVM medium and supplementation, and duration of in vitro culture, may also contribute towards differential gene expression in IVM oocytes. Another limitation is that, in our differential gene expression analysis, *p*-values (and not adjusted *p*-values) less than 0.05 were considered statistically significant. This lack of compensation may increase the frequency of false-positive results. However, we extracted the overlapping results with different analytical methods and datasets, which to some extent could reduce variability and provide relatively reliable results.

5. Conclusions

In summary, based on two independent datasets of IVM-MII oocytes, we identified hundreds of genes that were influenced by age, and that might be involved in the biological processes associated with cellular metabolism, DNA replication, and histone modifications. Among these age-related genes, *FAM111A* may act as a biomarker for oocyte aging, and deserves further investigation. Our findings could advance current knowledge of the molecular mechanisms involved in oocyte aging, and potentially facilitate the development of targeted treatments designed to improve oocyte quality.

Supplementary Materials: The following supporting information can be downloaded at: <https://www.mdpi.com/article/10.3390/biomedicines10020257/s1>. Table S1. Results of Spearman correlation on IVM-MII oocytes from Group I. IVM-MII, in vitro maturation-metaphase II; Table S2. Results of Spearman correlation on IVM-MII oocytes from Group II; Table S3. Results of *t*-test on IVM-MII oocytes from Group I; Table S4. Results of *t*-test on IVM-MII oocytes from Group II; Table S5. Results of GSEA analysis on IVM-MII oocytes from Group I. GSEA, Gene Set Enrichment Analysis; Table S6. Results of GSEA analysis on IVM-MII oocytes from Group II; Table S7. Results of GSEA analysis on IVM-MII oocytes from Group II. GSEA, Gene Set Variation Analysis.

Author Contributions: Conceptualization, U.J., V.v.S., T.K., M.K., S.M. (Sarah Meister); data analysis and visualization, H.Y., C.P., J.v.D., S.E.; Writing—original draft preparation, H.Y., C.P., J.v.D., S.E.; Writing—review and editing, M.K., C.K., M.R., C.H., S.G.F., G.W.; supervision, U.J., V.v.S., S.M. (Sven Mahner). All authors have read and agreed to the published version of the manuscript.

Funding: This research received no external funding.

Institutional Review Board Statement: Ethical review and approval were waived for this study, because all of the data used in the current study were anonymized data from GEO database.

Informed Consent Statement: Patient consent was waived because all of the data used in the current study were anonymized data from GEO database.

Data Availability Statement: Publicly available datasets were analyzed in this study. These data can be found here: GEO: <https://www.ncbi.nlm.nih.gov/geo/> (accessed on 15 November 2021).

Conflicts of Interest: The authors declare no conflict of interest.

References

- Dohle, G.R.; Colpi, G.M.; Hargreave, T.B.; Papp, G.K.; Jungwirth, A.; Weidner, W. EAU guidelines on male infertility. *Eur. Urol.* **2005**, *48*, 703–711. [[CrossRef](#)] [[PubMed](#)]
- Turan, V.; Oktay, K. BRCA-related ATM-mediated DNA double-strand break repair and ovarian aging. *Hum. Reprod. Update* **2020**, *26*, 43–57. [[CrossRef](#)] [[PubMed](#)]
- Baird, D.T.; Collins, J.; Egozcue, J.; Evers, L.H.; Gianaroli, L.; Leridon, H.; Sunde, A.; Templeton, A.; Van Steirteghem, A.; Cohen, J.; et al. Fertility and ageing ESHRE Capri Workshop Group. *Hum. Reprod. Update* **2005**, *11*, 261–276. [[CrossRef](#)] [[PubMed](#)]
- Marangos, P.; Stevance, M.; Niaka, K.; Lagoudaki, M.; Nabti, I.; Jessberger, R.; Carroll, J. DNA damage-induced metaphase I arrest is mediated by the spindle assembly checkpoint and maternal age. *Nat. Commun.* **2015**, *6*. [[CrossRef](#)] [[PubMed](#)]
- Keefe, D.L.; Niven-Fairchild, T.; Powell, S.; Buradagunta, S. Mitochondrial deoxyribonucleic acid deletions in oocytes and reproductive aging in women. *Fertil. Steril.* **1995**, *64*, 577–583. [[CrossRef](#)]
- Selesniemi, K.; Lee, H.J.; Muhlhauser, A.; Tilly, J.L. Prevention of maternal aging-associated oocyte aneuploidy and meiotic spindle defects in mice by dietary and genetic strategies. *Proc. Natl. Acad. Sci. USA* **2011**, *108*, 12319–12324. [[CrossRef](#)]
- Keefe, D.L.; Liu, L. Telomeres and reproductive aging. *Proc. Reprod. Fertil. Dev.* **2009**, *21*, 10–14. [[CrossRef](#)]
- Valeri, C.; Pappalardo, S.; De Felici, M.; Manna, C. Correlation of oocyte morphometry parameters with woman's age. *Proc. J. Assist. Reprod. Genet.* **2011**, *28*, 545–552. [[CrossRef](#)]
- Omidi, M.; Khalili, M.A.; Nahangi, H.; Ashourzadeh, S.; Rahimpour, M. Does women's age influence zona pellucida birefringence of metaphase II oocytes in in-vitro maturation program? *Int. J. Reprod. Biomed.* **2013**, *11*, 823–828.
- Duncan, F.E.; Jasti, S.; Paulson, A.; Kelsch, J.M.; Fegley, B.; Gerton, J.L. Age-associated dysregulation of protein metabolism in the mammalian oocyte. *Aging Cell* **2017**, *16*, 1381–1393. [[CrossRef](#)]
- Smits, M.A.J.; Wong, K.M.; Mantikou, E.; Korver, C.M.; Jongejan, A.; Breit, T.M.; Goddijn, M.; Mastenbroek, S.; Repping, S. Age-related gene expression profiles of immature human oocytes. *Mol. Hum. Reprod.* **2018**, *24*, 469–477. [[CrossRef](#)] [[PubMed](#)]
- Reyes, J.M.; Silva, E.; Chitwood, J.L.; Schoolcraft, W.B.; Krisher, R.L.; Ross, P.J. Differing molecular response of young and advanced maternal age human oocytes to IVM. *Hum. Reprod.* **2017**, *32*, 2199–2208. [[CrossRef](#)] [[PubMed](#)]
- Llonch, S.; Barragán, M.; Nieto, P.; Mallol, A.; Elosua-Bayes, M.; Lorden, P.; Ruiz, S.; Zambelli, F.; Heyn, H.; Vassena, R.; et al. Single human oocyte transcriptome analysis reveals distinct maturation stage-dependent pathways impacted by age. *Aging Cell* **2021**, *20*, e13360. [[CrossRef](#)] [[PubMed](#)]
- Grøndahl, M.L.; Yding Andersen, C.; Bogstad, J.; Nielsen, F.C.; Meinertz, H.; Borup, R. Gene expression profiles of single human mature oocytes in relation to age. *Hum. Reprod.* **2010**, *25*, 957–968. [[CrossRef](#)]
- Zhang, J.J.; Liu, X.; Chen, L.; Zhang, S.; Zhang, X.; Hao, C.; Miao, Y.L. Advanced maternal age alters expression of maternal effect genes that are essential for human oocyte quality. *Aging* **2020**, *12*, 3950–3961. [[CrossRef](#)]
- Yuan, L.; Yin, P.; Yan, H.; Zhong, X.; Ren, C.; Li, K.; Chin Heng, B.; Zhang, W.; Tong, G. Single-cell transcriptome analysis of human oocyte ageing. *J. Cell. Mol. Med.* **2021**, *25*, 6289–6303. [[CrossRef](#)]

17. Barragán, M.; Pons, J.; Ferrer-Vaquero, A.; Cornet-Bartolomé, D.; Schweitzer, A.; Hubbard, J.; Auer, H.; Rodoloso, A.; Vassena, R. The transcriptome of human oocytes is related to age and ovarian reserve. *Mol. Hum. Reprod.* **2017**, *23*, 535–548. [[CrossRef](#)]
18. Ritchie, M.E.; Phipson, B.; Wu, D.; Hu, Y.; Law, C.W.; Shi, W.; Smyth, G.K. Limma powers differential expression analyses for RNA-sequencing and microarray studies. *Nucleic Acids Res.* **2015**, *43*, e47. [[CrossRef](#)]
19. Bardou, P.; Mariette, J.; Escudie, F.; Djemiel, C.; Klopp, C. Jvenn: An interactive Venn diagram viewer. *BMC Bioinform.* **2014**, *15*, 293. [[CrossRef](#)]
20. Yu, G.; Wang, L.G.; Han, Y.; He, Q.Y. ClusterProfiler: An R package for comparing biological themes among gene clusters. *Omic J. Integr. Biol.* **2012**, *16*, 284–287. [[CrossRef](#)]
21. Villanueva, R.A.M.; Chen, Z.J. ggplot2: Elegant Graphics for Data Analysis (2nd ed.). *Meas. Interdiscip. Res. Perspect.* **2019**, *17*, 160–167. [[CrossRef](#)]
22. Walter, W.; Sánchez-Cabo, F.; Ricote, M. GOrplot: An R package for visually combining expression data with functional analysis. *Bioinformatics* **2015**, *31*, 2912–2914. [[CrossRef](#)] [[PubMed](#)]
23. Kassambara, A. ggpubr: “ggplot2” Based Publication Ready Plots. R Packag. Version 0.4.0 2020. Available online: <https://CRAN.R-project.org/package=ggpubr> (accessed on 9 August 2021).
24. Robin, X.; Turck, N.; Hainard, A.; Tiberti, N.; Lisacek, F.; Sanchez, J.C.; Müller, M. pROC: An open-source package for R and S+ to analyze and compare ROC curves. *BMC Bioinform.* **2011**, *12*, 77. [[CrossRef](#)] [[PubMed](#)]
25. Greiner, M.; Pfeiffer, D.; Smith, R.D. Principles and practical application of the receiver-operating characteristic analysis for diagnostic tests. *Prev. Vet. Med.* **2000**, *45*, 23–41. [[CrossRef](#)]
26. Subramanian, A.; Tamayo, P.; Mootha, V.K.; Mukherjee, S.; Ebert, B.L.; Gillette, M.A.; Paulovich, A.; Pomeroy, S.L.; Golub, T.R.; Lander, E.S.; et al. Gene set enrichment analysis: A knowledge-based approach for interpreting genome-wide expression profiles. *Proc. Natl. Acad. Sci. USA* **2005**, *102*, 15545–15550. [[CrossRef](#)]
27. Hänzelmann, S.; Castelo, R.; Guinney, J. GSEA: Gene set variation analysis for microarray and RNA-Seq data. *BMC Bioinform.* **2013**, *14*, 7. [[CrossRef](#)]
28. Franz, M.; Rodriguez, H.; Lopes, C.; Zuberi, K.; Montojo, J.; Bader, G.D.; Morris, Q. GeneMANIA update 2018. *Nucleic Acids Res.* **2018**, *46*, W60–W64. [[CrossRef](#)]
29. Warde-Farley, D.; Donaldson, S.L.; Comes, O.; Zuberi, K.; Badrawi, R.; Chao, P.; Franz, M.; Grouios, C.; Kazi, F.; Lopes, C.T.; et al. The GeneMANIA prediction server: Biological network integration for gene prioritization and predicting gene function. *Nucleic Acids Res.* **2010**, *38*, W214–W220. [[CrossRef](#)] [[PubMed](#)]
30. Leek, J.T.; Johnson, W.E.; Parker, H.S.; Jaffe, A.E.; Storey, J.D. The SVA package for removing batch effects and other unwanted variation in high-throughput experiments. *Bioinformatics* **2012**, *28*, 882–883. [[CrossRef](#)]
31. Wei, T.; Simko, V.; Levy, M.; Xie, Y.; Jin, Y.; Zemla, J. R package “corplot”: Visualization of a Correlation Matrix. *Statistician* **2017**, *56*, 316–324.
32. Catandi, G.D.; Obeidat, Y.M.; Broeckling, C.D.; Chen, T.W.; Chicco, A.J.; Carnevale, E.M. Equine maternal aging affects oocyte lipid content, metabolic function and developmental potential. *Reproduction* **2021**, *161*, 399–409. [[CrossRef](#)] [[PubMed](#)]
33. Sturme, R.G.; Reis, A.; Leese, H.J.; McEvoy, T.G. Role of fatty acids in energy provision during oocyte maturation and early embryo development. *Reprod. Domest. Anim.* **2009**, *44*, 50–58. [[CrossRef](#)] [[PubMed](#)]
34. McKeegan, P.J.; Sturme, R.G. The role of fatty acids in oocyte and early embryo development. *Reprod. Fertil. Dev.* **2012**, *24*, 59–67. [[CrossRef](#)] [[PubMed](#)]
35. Norwitz, E.R.; Schust, D.J.; Fisher, S.J. Implantation and the Survival of Early Pregnancy. *N. Engl. J. Med.* **2001**, *345*, 1400–1408. [[CrossRef](#)]
36. Sturme, R.G.; Leese, H.J. Energy metabolism in pig oocytes and early embryos. *Reproduction* **2003**, *126*, 197–204. [[CrossRef](#)]
37. Prates, E.G.; Nunes, J.T.; Pereira, R.M. A role of lipid metabolism during cumulus-oocyte complex maturation: Impact of lipid modulators to improve embryo production. *Mediat. Inflamm.* **2014**, *2014*, 692067. [[CrossRef](#)] [[PubMed](#)]
38. Prates, E.G.; Marques, C.C.; Baptista, M.C.; Vasques, M.I.; Carolino, N.; Horta, A.E.M.; Chameca, R.; Nunes, J.T.; Pereira, R.M. Fat area and lipid droplet morphology of porcine oocytes during in vitro maturation with trans-10, cis-12 conjugated linoleic acid and forskolin. *Animal* **2013**, *7*, 602–609. [[CrossRef](#)]
39. Prates, E.G.; Alves, S.P.; Marques, C.C.; Baptista, M.C.; Horta, A.E.M.; Bessa, R.J.B.; Pereira, R.M. Fatty acid composition of porcine cumulus oocyte complexes (COC) during maturation: Effect of the lipid modulators trans-10, cis-12 conjugated linoleic acid (t10, c12 CLA) and forskolin. *Vitr. Cell. Dev. Biol.-Anim.* **2013**, *49*, 335–345. [[CrossRef](#)]
40. Bradley, J.; Swann, K. Mitochondria and lipid metabolism in mammalian oocytes and early embryos. *Int. J. Dev. Biol.* **2019**, *63*, 93–103. [[CrossRef](#)]
41. Manosalva, I.; González, A. Aging changes the chromatin configuration and histone methylation of mouse oocytes at germinal vesicle stage. *Theriogenology* **2010**, *74*, 1539–1547. [[CrossRef](#)]
42. Shao, G.B.; Wang, J.; Zhang, L.P.; Wu, C.Y.; Jin, J.; Sang, J.R.; Lu, H.Y.; Gong, A.H.; Du, F.Y.; Peng, W.X. Aging alters histone H3 lysine 4 methylation in mouse germinal vesicle stage oocytes. *Reprod. Fertil. Dev.* **2015**, *27*, 419–426. [[CrossRef](#)] [[PubMed](#)]
43. Huang, J.C.; Yan, L.Y.; Lei, Z.L.; Miao, Y.L.; Shi, L.H.; Yang, J.W.; Wang, Q.; Ouyang, Y.C.; Sun, Q.Y.; Chen, D.Y. Changes in histone acetylation during postovulatory aging of mouse oocyte. *Biol. Reprod.* **2007**, *77*, 666–670. [[CrossRef](#)] [[PubMed](#)]

44. Suo, L.; Meng, Q.G.; Pei, Y.; Yan, C.L.; Fu, X.W.; Bunch, T.D.; Zhu, S.E. Changes in acetylation on lysine 12 of histone H4 (acH4K12) of murine oocytes during maternal aging may affect fertilization and subsequent embryo development. *Fertil. Steril.* **2010**, *93*, 945–951. [[CrossRef](#)] [[PubMed](#)]
45. Manosalva, I.; González, A. Aging alters histone H4 acetylation and CDC2A in mouse germinal vesicle stage oocytes. *Biol. Reprod.* **2009**, *81*, 1164–1171. [[CrossRef](#)] [[PubMed](#)]
46. Yang, H.; Ma, Z.; Peng, L.; Kuhn, C.; Rahmeh, M.; Mahner, S.; Jeschke, U.; von Schönfeldt, V. Comparison of histone h3k4me3 between ivf and icisi technologies and between boy and girl offspring. *Int. J. Mol. Sci.* **2021**, *22*, 8574. [[CrossRef](#)]
47. Gonzalo, S.; Blasco, M.A. Role of Rb family in the epigenetic definition of chromatin. *Cell Cycle* **2005**, *4*, 752–755. [[CrossRef](#)]
48. Pontelo, T.P.; Franco, M.M.; Kawamoto, T.S.; Caixeta, F.M.C.; de Oliveira Leme, L.; Kussano, N.R.; Zangeronimo, M.G.; Dode, M.A.N. Histone deacetylase inhibitor during in vitro maturation decreases developmental capacity of bovine oocytes. *PLoS ONE* **2021**, *16*, e0247518. [[CrossRef](#)]
49. Cypris, O.; Eipel, M.; Franzen, J.; Rösseler, C.; Tharmapalan, V.; Kuo, C.C.; Vieri, M.; Nikolić, M.; Kirschner, M.; Brümmendorf, T.H.; et al. PRDM8 reveals aberrant DNA methylation in aging syndromes and is relevant for hematopoietic and neuronal differentiation. *Clin. Epigenetics* **2020**, *12*, 125. [[CrossRef](#)]
50. Steuerwald, N.M.; Bermúdez, M.G.; Wells, D.; Munné, S.; Cohen, J. Maternal age-related differential global expression profiles observed in human oocytes. *Reprod. Biomed. Online* **2007**, *14*, 700–708. [[CrossRef](#)]
51. Fine, D.A.; Rozenblatt-Rosen, O.; Padi, M.; Korkhin, A.; James, R.L.; Adelmant, G.; Yoon, R.; Guo, L.; Berrios, C.; Zhang, Y.; et al. Identification of FAM111A as an SV40 Host Range Restriction and Adenovirus Helper Factor. *PLoS Pathog.* **2012**, *8*, e1002949. [[CrossRef](#)]
52. Kojima, Y.; Machida, Y.; Palani, S.; Caulfield, T.R.; Radisky, E.S.; Kaufmann, S.H.; Machida, Y.J. FAM111A protects replication forks from protein obstacles via its trypsin-like domain. *Nat. Commun.* **2020**, *11*, 1318. [[CrossRef](#)] [[PubMed](#)]
53. Rios-Szwed, D.O.; Garcia-Wilson, E.; Sanchez-Pulido, L.; Alvarez, V.; Jiang, H.; Bandau, S.; Lamond, A.; Ponting, C.P.; Alabert, C. FAM111A regulates replication origin activation and cell fitness. *BioRxiv* **2020**, 1–26. [[CrossRef](#)]
54. Nie, M.; Oravcová, M.; Jami-Alahmadi, Y.; Wohlschlegel, J.A.; Lazzarini-Denchi, E.; Boddy, M.N. FAM111A induces nu-clear dysfunction in disease and viral restriction. *EMBO Rep.* **2021**, *22*, e50803. [[CrossRef](#)] [[PubMed](#)]
55. Alabert, C.; Bukowski-Wills, J.C.; Lee, S.B.; Kustatscher, G.; Nakamura, K.; De Lima Alves, F.; Menard, P.; Mejlvang, J.; Rappsilber, J.; Groth, A. Nascent chromatin capture proteomics determines chromatin dynamics during DNA replication and identifies unknown fork components. *Nat. Cell Biol.* **2014**, *16*, 281–291. [[CrossRef](#)] [[PubMed](#)]
56. Lee, A.W.T.; Ng, J.K.W.; Liao, J.; Luk, A.C.; Suen, A.H.C.; Chan, T.T.H.; Cheung, M.Y.; Chu, H.T.; Tang, N.L.S.; Zhao, M.P.; et al. Single-cell RNA sequencing identifies molecular targets associated with poor in vitro maturation performance of oocytes collected from ovarian stimulation. *Hum. Reprod.* **2021**, *36*, 1907–1921. [[CrossRef](#)] [[PubMed](#)]
57. Pamarthy, S.; Kulshrestha, A.; Katara, G.K.; Beaman, K.D. The curious case of vacuolar ATPase: Regulation of signaling pathways. *Mol. Cancer* **2018**, *17*, 41. [[CrossRef](#)]
58. Liu, C.F.; Parker, K.; Humphrey, Y. WNT4/ β -catenin pathway maintains female germ cell survival by inhibiting activin β B in the mouse fetal ovary. *PLoS ONE* **2010**, *5*, e10382. [[CrossRef](#)]
59. Polakis, P. Wnt signaling in cancer. *Cold Spring Harb. Perspect. Biol.* **2012**, *4*, 9. [[CrossRef](#)]
60. Miller, J.R. The Wnts. *Genome Biol.* **2002**, *3*, reviews3001.1. [[CrossRef](#)]
61. Cadigan, K.M.; Nusse, R. Wnt signaling: A common theme in animal development. *Genes Dev.* **1997**, *11*, 3286–3305. [[CrossRef](#)]
62. Moldovan, G.L.; Pfander, B.; Jentsch, S. PCNA, the Maestro of the Replication Fork. *Cell* **2007**, *129*, 665–679. [[CrossRef](#)] [[PubMed](#)]
63. Cazzalini, O.; Sommatos, S.; Tillhon, M.; Dutto, I.; Bachi, A.; Rapp, A.; Nardo, T.; Scovassi, A.I.; Necchi, D.; Cardoso, M.C.; et al. CBP and p300 acetylate PCNA to link its degradation with nucleotide excision repair synthesis. *Nucleic Acids Res.* **2014**, *42*, 8433–8448. [[CrossRef](#)] [[PubMed](#)]
64. Persikov, A.V.; Rowland, E.F.; Oakes, B.L.; Singh, M.; Noyes, M.B. Deep sequencing of large library selections allows computational discovery of diverse sets of zinc fingers that bind common targets. *Nucleic Acids Res.* **2014**, *42*, 1497–1508. [[CrossRef](#)] [[PubMed](#)]
65. Yang, H.; Kolben, T.; Meister, S.; Paul, C.; van Dorp, J.; Eren, S.; Kuhn, C.; Rahmeh, M.; Mahner, S.; Jeschke, U.; et al. Factors Influencing the In Vitro Maturation (IVM) of Human Oocyte. *Biomedicines.* **2021**, *9*, 1904. [[CrossRef](#)]

Huixia Yang, Thomas Kolben, Mirjana Kessler, Sarah Meister, Corinna Paul, Julia van Dorp, Sibel Eren, Christina Kuhn, Martina Rahmeh, Cornelia Herbst, Sabine Gabriele Fink, Gabriele Weimer, Sven Mahner, Udo Jeschke, Viktoria von Schönfeldt. *FAM111A* Is a Novel Molecular Marker for Oocyte Aging. *Biomedicines.* 2022 Jan 25;10(2):257. doi: 10.3390/biomedicines10020257.

References

1. Reynolds N, Collier B, Maratou K, Bingham V, Speed RM, Taggart M, Semple CA, Gray NK, Cooke HJ. Dazl binds in vivo to specific transcripts and can regulate the pre-meiotic translation of Mvh in germ cells. *Hum Mol Genet.* 2005 Dec 15;14(24):3899-909. doi: 10.1093/hmg/ddi414.
2. Tuerlings JH, de France HF, Hamers A, Hordijk R, Van Hemel JO, Hansson K, Hoovers JM, Madan K, Van der Blij-Philipsen M, Gerssen-Schoorl KB, Kremer JA, Smeets DF. Chromosome studies in 1792 males prior to intra-cytoplasmic sperm injection: the Dutch experience. *Eur J Hum Genet.* 1998 May-Jun;6(3):194-200. doi: 10.1038/sj.ejhg.5200193.
3. Ma RCW, Ng NYH, Cheung LP. Assisted reproduction technology and long-term cardiometabolic health in the offspring. *PLoS Med.* 2021 Sep 7;18(9):e1003724. doi: 10.1371/journal.pmed.1003724.
4. Pisarska MD, Chan JL, Lawrenson K, Gonzalez TL, Wang ET. Genetics and Epigenetics of Infertility and Treatments on Outcomes. *J Clin Endocrinol Metab.* 2019 Jun 1;104(6):1871-1886. doi: 10.1210/jc.2018-01869.
5. Horsthemke B, Ludwig M. Assisted reproduction: the epigenetic perspective. *Hum Reprod Update.* 2005 Sep-Oct;11(5):473-82. doi: 10.1093/humupd/dmi022. Epub 2005 Jul 1.
6. Chang HY, Hwu WL, Chen CH, Hou CY, Cheng W. Children Conceived by Assisted Reproductive Technology Prone to Low Birth Weight, Preterm Birth, and Birth Defects: A Cohort Review of More Than 50,000 Live Births During 2011-2017 in Taiwan. *Front Pediatr.* 2020 Mar 13;8:87. doi: 10.3389/fped.2020.00087.
7. Dar S, Librach CL, Gunby J, Bissonnette F, Cowan L; IVF Directors Group of Canadian Fertility and Andrology Society. Increased risk of preterm birth in singleton pregnancies after blastocyst versus Day 3 embryo transfer: Canadian ART Register (CARTR) analysis. *Hum Reprod.* 2013 Apr;28(4):924-8. doi: 10.1093/humrep/des448.

8. Yang X, Li Y, Li C, Zhang W. Current overview of pregnancy complications and live-birth outcome of assisted reproductive technology in mainland China. *Fertil Steril*. 2014 Feb;101(2):385-91. doi: 10.1016/j.fertnstert.2013.10.017.
9. Hattori H, Hiura H, Kitamura A, Miyauchi N, Kobayashi N, Takahashi S, Okae H, Kyono K, Kagami M, Ogata T, Arima T. Association of four imprinting disorders and ART. *Clin Epigenetics*. 2019 Feb 7;11(1):21. doi: 10.1186/s13148-019-0623-3.
10. Sutcliffe AG, Peters CJ, Bowdin S, Temple K, Reardon W, Wilson L, Clayton-Smith J, Brueton LA, Bannister W, Maher ER. Assisted reproductive therapies and imprinting disorders--a preliminary British survey. *Hum Reprod*. 2006 Apr;21(4):1009-11. doi: 10.1093/humrep/dei405.
11. Demars J, Shmela ME, Rossignol S, Okabe J, Netchine I, Azzi S, Cabrol S, Le Caignec C, David A, Le Bouc Y, El-Osta A, Gicquel C. Analysis of the IGF2/H19 imprinting control region uncovers new genetic defects, including mutations of OCT-binding sequences, in patients with 11p15 fetal growth disorders. *Hum Mol Genet*. 2010 Mar 1;19(5):803-14. doi: 10.1093/hmg/ddp549.
12. Poole RL, Leith DJ, Docherty LE, Shmela ME, Gicquel C, Splitt M, Temple IK, Mackay DJ. Beckwith-Wiedemann syndrome caused by maternally inherited mutation of an OCT-binding motif in the IGF2/H19-imprinting control region, ICR1. *Eur J Hum Genet*. 2012 Feb;20(2):240-3. doi: 10.1038/ejhg.2011.166.
13. Robbins KM, Chen Z, Wells KD, Rivera RM. Expression of KCNQ1OT1, CDKN1C, H19, and PLAGL1 and the methylation patterns at the KvDMR1 and H19/IGF2 imprinting control regions is conserved between human and bovine. *J Biomed Sci*. 2012 Nov 15;19(1):95. doi: 10.1186/1423-0127-19-95.
14. Maher ER, Brueton LA, Bowdin SC, Luharia A, Cooper W, Cole TR, Macdonald F, Sampson JR, Barratt CL, Reik W, Hawkins MM. Beckwith-Wiedemann syndrome and assisted reproduction technology (ART). *J Med Genet*. 2003 Jan;40(1):62-4. doi: 10.1136/jmg.40.1.62. Erratum in: *J Med Genet*. 2003 Apr;40(4):304.
15. Wilkins-Haug L. Epigenetics and assisted reproduction. *Curr Opin Obstet Gynecol*. 2009 Jun;21(3):201-6. doi: 10.1097/GCO.0b013e32832d7b95.
16. Pastuzyn ED, Shepherd JD. Activity-Dependent Arc Expression and Homeostatic Synaptic Plasticity Are Altered in Neurons from a Mouse Model of An-

- gelman Syndrome. *Front Mol Neurosci*. 2017 Jul 28;10:234. doi: 10.3389/fnmol.2017.00234.
17. Whitelaw N, Bhattacharya S, Hoad G, Horgan GW, Hamilton M, Haggarty P. Epigenetic status in the offspring of spontaneous and assisted conception. *Hum Reprod*. 2014 Jul;29(7):1452-8. doi: 10.1093/humrep/deu094.
 18. Wang Y, Yuan P, Yan Z, Yang M, Huo Y, Nie Y, Zhu X, Qiao J, Yan L. Single-cell multiomics sequencing reveals the functional regulatory landscape of early embryos. *Nat Commun*. 2021 Feb 23;12(1):1247. doi: 10.1038/s41467-021-21409-8.
 19. Huntriss J, Balen AH, Sinclair KD, Brison DR, Picton HM; Royal College of Obstetricians Gynaecologists. Epigenetics and Reproductive Medicine: Scientific Impact Paper No. 57. *BJOG*. 2018 Dec;125(13):e43-e54. doi: 10.1111/1471-0528.15240.
 20. Tomizawa S, Nowacka-Woszek J, Kelsey G. DNA methylation establishment during oocyte growth: mechanisms and significance. *Int J Dev Biol*. 2012;56(10-12):867-75. doi: 10.1387/ijdb.120152gk.
 21. Sato A, Otsu E, Negishi H, Utsunomiya T, Arima T. Aberrant DNA methylation of imprinted loci in superovulated oocytes. *Hum Reprod*. 2007 Jan;22(1):26-35. doi: 10.1093/humrep/del316.
 22. Kobayashi H, Hiura H, John RM, Sato A, Otsu E, Kobayashi N, Suzuki R, Suzuki F, Hayashi C, Utsunomiya T, Yaegashi N, Arima T. DNA methylation errors at imprinted loci after assisted conception originate in the parental sperm. *Eur J Hum Genet*. 2009 Dec;17(12):1582-91. doi: 10.1038/ejhg.2009.68.
 23. Cao B, Parnell LA, Diamond MS, Mysorekar IU. Inhibition of autophagy limits vertical transmission of Zika virus in pregnant mice. *J Exp Med*. 2017 Aug 7;214(8):2303-2313. doi: 10.1084/jem.20170957.
 24. Barker DJ, Bull AR, Osmond C, Simmonds SJ. Fetal and placental size and risk of hypertension in adult life. *BMJ*. 1990 Aug 4;301(6746):259-62. doi: 10.1136/bmj.301.6746.259.
 25. Lesseur C, Chen J. Adverse Maternal Metabolic Intrauterine Environment and Placental Epigenetics: Implications for Fetal Metabolic Programming. *Curr Environ Health Rep*. 2018 Dec;5(4):531-543. doi: 10.1007/s40572-018-0217-9.

26. Fall CHD, Kumaran K. Metabolic programming in early life in humans. *Philos Trans R Soc Lond B Biol Sci.* 2019 Apr 15;374(1770):20180123. doi: 10.1098/rstb.2018.0123.
27. Xiang M, Chen S, Zhang X, Ma Y. Placental diseases associated with assisted reproductive technology. *Reprod Biol.* 2021 Jun;21(2):100505. doi: 10.1016/j.repbio.2021.100505.
28. Choux C, Ginod P, Barberet J, Rousseau T, Bruno C, Sagot P, Astruc K, Fauque P. Placental volume and other first-trimester outcomes: are there differences between fresh embryo transfer, frozen-thawed embryo transfer and natural conception? *Reprod Biomed Online.* 2019 Apr;38(4):538-548. doi: 10.1016/j.rbmo.2018.12.023.
29. Menelaou K, Prater M, Tunster SJ, Blake GET, Geary Joo C, Cross JC, Hamilton RS, Watson ED. Blastocyst transfer in mice alters the placental transcriptome and growth. *Reproduction.* 2020 Feb;159(2):115-132. doi: 10.1530/REP-19-0293.
30. Cochrane E, Pando C, Kirschen GW, Soucier D, Fuchs A, Garry DJ. Assisted reproductive technologies (ART) and placental abnormalities. *J Perinat Med.* 2020 Oct 25;48(8):825-828. doi: 10.1515/jpm-2020-0141.
31. Romundstad LB, Romundstad PR, Sunde A, von Düring V, Skjaerven R, Vatlen LJ. Increased risk of placenta previa in pregnancies following IVF/ICSI; a comparison of ART and non-ART pregnancies in the same mother. *Hum Reprod.* 2006 Sep;21(9):2353-8. doi: 10.1093/humrep/del153.
32. Haavaldsen C, Tanbo T, Eskild A. Placental weight in singleton pregnancies with and without assisted reproductive technology: a population study of 536,567 pregnancies. *Hum Reprod.* 2012 Feb;27(2):576-82. doi: 10.1093/humrep/der428.
33. Rhon-Calderon EA, Vrooman LA, Riesche L, Bartolomei MS. The effects of Assisted Reproductive Technologies on genomic imprinting in the placenta. *Placenta.* 2019 Sep 1;84:37-43. doi: 10.1016/j.placenta.2019.02.013.
34. St-Pierre J, Hivert MF, Perron P, Poirier P, Guay SP, Brisson D, Bouchard L. IGF2 DNA methylation is a modulator of newborn's fetal growth and development. *Epigenetics.* 2012 Oct;7(10):1125-32. doi: 10.4161/epi.21855.

35. Argyraki M, Damdimopoulou P, Chatzimeletiou K, Grimbizis GF, Tarlatzis BC, Syrrou M, Lambropoulos A. In-utero stress and mode of conception: impact on regulation of imprinted genes, fetal development and future health. *Hum Reprod Update*. 2019 Nov 5;25(6):777-801. doi: 10.1093/humupd/dmz025.
36. Sakian S, Louie K, Wong EC, Havelock J, Kashyap S, Rowe T, Taylor B, Ma S. Altered gene expression of H19 and IGF2 in placentas from ART pregnancies. *Placenta*. 2015 Oct;36(10):1100-5. doi: 10.1016/j.placenta.2015.08.008.
37. Wang YX, Yue LF, Zhang JW, Xiong YW, Hu JJ, Wang LL, Li Z, Liu Y, Yang L, Sun LJ. Expression and DNA Methylation Status of the Imprinted Genes PEG10 and L3MBTL1 in the Umbilical Cord Blood and Placenta of the Offspring of Assisted Reproductive Technology. *Reprod Sci*. 2021 Apr;28(4):1133-1141. doi: 10.1007/s43032-020-00417-x.
38. de Waal E, Vrooman LA, Fischer E, Ord T, Mainigi MA, Coutifaris C, Schultz RM, Bartolomei MS. The cumulative effect of assisted reproduction procedures on placental development and epigenetic perturbations in a mouse model. *Hum Mol Genet*. 2015 Dec 15;24(24):6975-85. doi: 10.1093/hmg/ddv400.
39. de Waal E, Mak W, Calhoun S, Stein P, Ord T, Krapp C, Coutifaris C, Schultz RM, Bartolomei MS. In vitro culture increases the frequency of stochastic epigenetic errors at imprinted genes in placental tissues from mouse concepti produced through assisted reproductive technologies. *Biol Reprod*. 2014 Feb 6;90(2):22. doi: 10.1095/biolreprod.113.114785.
40. Newman JE, Paul RC, Chambers GM. Assisted reproductive technology in Australia and New Zealand 2018. Sydney, Australia: National Perinatal Epidemiology and Statistics Unit, University of New South Wales. 2019.
41. Miao YL, Kikuchi K, Sun QY, Schatten H. Oocyte aging: cellular and molecular changes, developmental potential and reversal possibility. *Hum Reprod Update*. 2009 Sep-Oct;15(5):573-85. doi: 10.1093/humupd/dmp014.
42. Smits MAJ, Wong KM, Mantikou E, Korver CM, Jongejan A, Breit TM, Goddijn M, Mastenbroek S, Repping S. Age-related gene expression profiles of immature human oocytes. *Mol Hum Reprod*. 2018 Oct 1;24(10):469-477. doi: 10.1093/molehr/gay036.
43. Reyes JM, Silva E, Chitwood JL, Schoolcraft WB, Krisher RL, Ross PJ. Differing molecular response of young and advanced maternal age human oocytes

- to IVM. *Hum Reprod.* 2017 Nov 1;32(11):2199-2208. doi: 10.1093/humrep/dex284.
44. Llonch S, Barragán M, Nieto P, Mallof A, Elosua-Bayes M, Lorden P, Ruiz S, Zambelli F, Heyn H, Vassena R, Payer B. Single human oocyte transcriptome analysis reveals distinct maturation stage-dependent pathways impacted by age. *Aging Cell.* 2021 May;20(5):e13360. doi: 10.1111/accel.13360.
45. Grøndahl ML, Yding Andersen C, Bogstad J, Nielsen FC, Meinertz H, Borup R. Gene expression profiles of single human mature oocytes in relation to age. *Hum Reprod.* 2010 Apr;25(4):957-68. doi: 10.1093/humrep/deq014.
46. Barragán M, Pons J, Ferrer-Vaquero A, Cornet-Bartolomé D, Schweitzer A, Hubbard J, Auer H, Rodoloso A, Vassena R. The transcriptome of human oocytes is related to age and ovarian reserve. *Mol Hum Reprod.* 2017 Aug 1;23(8):535-548. doi: 10.1093/molehr/gax033.
47. Xu L, Yu W, Xiao H, Lin K. BIRC5 is a prognostic biomarker associated with tumor immune cell infiltration. *Sci Rep.* 2021 Jan 11;11(1):390. doi: 10.1038/s41598-020-79736-7.
48. Zhong Q, Kowluru RA. Regulation of matrix metalloproteinase-9 by epigenetic modifications and the development of diabetic retinopathy. *Diabetes.* 2013 Jul;62(7):2559-68. doi: 10.2337/db12-1141.
49. Sermon, Karen, and Stéphane Viville, eds. *Textbook of Human Reproductive Genetics*. Cambridge University Press, 2014. Chapter 12, 172 页
50. Kämpf C, Specht M, Scholz A, Puppel SH, Doose G, Reiche K, Schor J, Hackermüller J. uap: reproducible and robust HTS data analysis. *BMC Bioinformatics.* 2019 Dec 12;20(1):664. doi: 10.1186/s12859-019-3219-1.
51. Zhang XL, Wu J, Wang J, Shen T, Li H, Lu J, Gu Y, Kang Y, Wong CH, Ngan CY, Shao Z, Wu J, Zhao X. Integrative epigenomic analysis reveals unique epigenetic signatures involved in unipotency of mouse female germline stem cells. *Genome Biol.* 2016 Jul 27;17(1):162. doi: 10.1186/s13059-016-1023-z.
52. Dambacher S, Hahn M, Schotta G. Epigenetic regulation of development by histone lysine methylation. *Heredity (Edinb).* 2010 Jul;105(1):24-37. doi: 10.1038/hdy.2010.49.
53. Fan X, Zhang X, Wu X, Guo H, Hu Y, Tang F, Huang Y. Single-cell RNA-seq transcriptome analysis of linear and circular RNAs in mouse preimplantation

- embryos. *Genome Biol.* 2015 Jul 23;16(1):148. doi: 10.1186/s13059-015-0706-1.
54. Müller-Platz C. Misuse potential of molecular biology and biotechnology in sport. *Drug Test Anal.* 2011 Oct;3(10):643-4. doi: 10.1002/dta.353.
55. Wang Z, Gerstein M, Snyder M. RNA-Seq: a revolutionary tool for transcriptomics. *Nat Rev Genet.* 2009 Jan;10(1):57-63. doi: 10.1038/nrg2484.

Acknowledgements

I would like to first express my deep and sincere gratitude to Prof. Udo Jeschke and Dr. Viktoria von Schönfeldt, for their great supervision for my doctoral thesis! To Prof. Udo Jeschke, I would like to extend my gratitude to him for introducing me to the field of scientific research and giving me deeper insight into how to carry out scientific research. I am lucky to have met such an approachable supervisor with formidable erudition. Under his guidance, my scientific research skills have more than significantly improved in just these few years. I also want to extend my sincere gratitude to Dr. Viktoria von Schönfeldt for her scientific research guidance. In addition, Dr. Viktoria von Schönfeldt's care and thoughtfulness toward me were as deep as a mother's. My heart is full of gratitude towards her for what she has done for me as a supervisor.

I also feel thankful to Prof. Thomas Kolben and Prof. Artur Mayerhofer from my Thesis Advisory Committee for their instruction on my thesis. I still remember when I entered the Ludwig Maximilian University of Munich (LMU), and Prof. Artur Mayerhofer kindly helped me to sign my admission formalities even though he was busy with his work. His style and gentleness have given my perturbed heart instant relief.

Thanks to Prof. Sven Mahner, Dr. Mirjana Kessler, Dr. Anca Chelariu-Raicu, Christina Kuhn, Martina Rahmeh, Cornelia Herbst, Sabine Gabriele Fink, and Gabriele Weimer for their support and guidance on my experiments. Also, thanks to my fellow students Corinna Paul, Julia van Dorp, and Sibel Eren for kindly teaching me how to isolate primary cells from human placenta and how to

analyze cells via flow cytometry in the past year. Although the relevant research contents are not reported in this doctoral thesis, I obtained deeper insight into the scientific research in the field of Obstetrics and Gynecology. I would also like to thank all other fellow students in lab. During the process of completing my doctoral project, I asked many questions about research, but they always responded to me eagerly with open arms and shared their experience and methods with me. I am grateful to all of them, and they are unforgettable.

Moreover, thanks to the education and instruction at LMU Munich. My doctoral life at LMU Munich has been a very fulfilling and fruitful journey. I have learned not only how to do scientific research, but also how to take care of myself. For me, this period of life has been very beautiful and will be one of my most valuable life experiences and a precious time.

Finally, I would like to thank my beloved family for sharing the joys of life with me on my road through life and showing me selfless love and unconditional support and encouragement. This gratitude will certainly fertilize my motivation to work harder in the future and I will repay all your love and support.

I sincerely wish my supervisors, colleagues, and fellow students who worked together with me in the last few years, my beloved family, and also myself all the best in our future lives and work.